April 2019

Dynamic Pricing of Electricity and Demand Response in Smart Communities

Vignesh Subramanian
University of South Florida, vignesh3587@gmail.com

Dynamic Pricing of Electricity and Demand Response in Smart Communities

by

Vignesh Subramanian

A dissertation submitted in partial fulfillment
of the requirements for the degree of
Doctor of Philosophy
Department of Industrial and Management Systems Engineering
College of Engineering
University of South Florida

Major Professor: Tapas K. Das, Ph.D.
Andrei Barbos, Ph.D.
Changhyun Kwon, Ph.D.
Hadi Charkhgard, Ph.D.
Zhixin Miao, Ph.D.

Date of Approval:
March 28, 2019

Keywords: aggregated demand response, electric vehicles, mathematical program with equilibrium constraints, robust optimization

DEDICATION

I dedicate this dissertation to my parents, friends and to all who encouraged me along the way.

ACKNOWLEDGMENTS

I would like to thank my advisor Dr. Tapas K. Das, for his guidance, motivation and continued support over the years. Most importantly spending time on weekends and after work hours to write our research papers. I couldn't imagine having a better mentor for my Ph.D. study. I would also like to thank my thesis dissertation members for all their insightful comments and suggestions.

I thank all my fellow graduate students, friends from Tampa, and Ivy oaks group for making my stay in Florida more memorable and kept me smiling the whole time.

TABLE OF CONTENTS

ABSTRACT

Grid modernization using advanced metering infrastructure (AMI) will continue to enhance timely communication among the system operator (SO), producers, and consumers. This will further empower the vision of dynamic pricing and demand side management (DSM). The phrase *dynamic pricing* in this dissertation refers to the practice of disclosing binding prices of electricity just ahead of consumption. As regards DSM, the focus is on collective demand response (DR) by aggregators managing consumers' loads in smart and connected communities (households, businesses, industries and aggregation of electric vehicle batteries). However, practitioners and researchers alike have expressed the fear that dynamic pricing may cause wild fluctuations in demand, which in turn will adversely affect both the network and market. To dispel this common apprehension and to show that it is possible to treat electricity as any other commodity (where binding prices are declared before consumption), there is a need to develop complementary policies for dynamic pricing decision by SOs and DR actions by load aggregators.

The overarching goal of this dissertation is to examine if it is viable to trade electricity like other commodities, where price is declared in advance and allows the consumers to engage in price responsive demand response actions. To achieve this, two different approaches are developed, one using data driven learning approach and the other using a two-level game theoretical framework. Thereafter, demonstrate both approaches are implemented on a sample interconnected power network and their benefits are highlighted. In the first approach, a comprehensive agent-based methodology guided by data-driven learning model is developed to derive stable and coordinated strategies for dynamic pricing and demand response in smart and connected communities. This

methodology is intended to support the policy makers in understanding the joint impact of: 1) the bidding behavior of power producers 2) dynamic pricing by the SO, and 3) DR actions by aggregators managing a variety of consumer loads.

The second approach is based on a robust game-theoretic framework with a two-layer optimization model. The top-layer is a two-stage stochastic model to address day-ahead decisions and the bottom-layer is a robust bilevel model that yields real-time actions comprising hourly dynamic prices by SO and optimal demand response by the aggregators. The two-layer model aims to minimize the cost to consumers while also maintaining SO's revenue neutral status in the presence of price spikes in the real-time markets.

The final component of this dissertation study focuses on the critical aspects of minimizing disruption in power networks under extreme weather events. An algorithm is presented that allows for optimal islanding of power network to limit the failure propagation during extreme events.

CHAPTER 1: INTRODUCTION

1.1 Background

Before proceeding to examine the potential of DR in the presence of dynamic pricing policies, it is important to understand the nature of existing power market structure.

1.1.1 Fundamentals of Power Market

In contrast to most other commodities, holding or storage of electricity is not economically viable, which implies that electricity should be supplied only as demanded. In a power network, SO is primarily responsible to match the supply and demand of electricity at all instants of time, which is also essential for a network to operate in a secure and reliable manner. The consumers' demand changes from time to time and accurate forecasting of future demand is complex. As a result, a wide range of generation mix are employed to meet the demand. For example, base load generators with a low operating cost generally used are in the network to satisfy the projected load. Any increase in demand from the projected loads are met by the peaking generators with a quick start but high cost. Prior to deregulation of electricity market, a traditional market structure commonly known as a *Vertically Integrated Market* was used for energy transactions. In this market, the SO or the utilities procure energy capacities from the generating parties at a price decided by state service commission's rate-making regulation [1]. In such a scheme, the actual cost of generation is known only to individual parties or utilities, not to the public. To make the power markets more competitive, markets were restructured/deregulated, where the privatized electricity providers are allowed to compete with each other to sell electricity to the SO. This opened up a wholesale market in which at different time periods competing generators place their supply price

bids and energy quantities to SO. The SO, through a merit order dispatch, selects the supply bids to match the projected demand and hourly market prices at the nodes are set by the highest market clearing bid.

1.1.2 Challenges and Opportunities in Deregulated Power Market

After deregulation, the power markets found an increased interest among suppliers to compete in the wholesale electricity market. Most of the deregulated markets adopt a two-settlement strategy: 1) day-ahead market, where SO receives the projected demand for the following day and schedules hourly quantities for the selected suppliers, 2) real-time market, which is used to settle any deviation from the day-ahead demand at the time of dispatch and the needed quantity is purchased from suppliers' who bid in real-time market. If either unexpected high demand and/or loss of generation capacity occur at the time of dispatch, this causes price spikes in the real time market. Typically, reserve capacities are maintained to overcome the above extreme events. A challenge of the power market is that these reserve capacities stay idle most of the time in the network. It is estimated that 10% of the annual energy cost is incurred in 1% of the operating time due to demand peaking resulting price spikes [2]. Another challenge faced by the deregulation is market arbitrage, where suppliers withhold a portion of their generation capacity from bidding. As a result, the high cost supplier is selected in the market who sets the market price. To overcome the above challenges of reserve capacity needs and capacity withholdings, policy makers recognized that DR has the potential to address both. As reported in [3], even slight demand side participation can significantly reduce the wholesale electricity prices, thus reducing market power of the producers. Also, DR assisted balancing of consumer demand can ease the burden of current practice of maintaining peaking generation capacity at the level of 10 - 15% of the expected demand [4].

1.1.3 Evolution of Demand Response

DR has been viewed as a key element to improve power market operations. Lack of DR is attributed to price spikes in real-time market, increased need of reserve capacity, suppliers' arbitrage, and network reliability issues. There are two supporting rationale in power markets to engage consumers in DR practices. The first is to give financial incentives for any load reduction offered by consumers and the second one is allowing the electricity tariff rate to change at each time interval following the market conditions. DR has traditionally been used as an emergency service provider in the event of peak load and/or outages. The primary participants in this DR programs has been either industrial loads or huge commercial loads. Due to lack of infrastructure and technologies, as well as little access to information, the residential consumers are currently unable to participate in DR programs. Per prevailing practice, the utilities or SO interrupts the residential loads directly from the dispatch control center on short notice. But, such practices failed to encourage the consumer to engage in DR programs. Practitioners and researchers argued that implementation of full-fledged DR programs will require advanced metering infrastructure [5], favorable regulatory reforms [6] and proper pricing practices [7].

1.1.4 Challenges and Opportunities of Demand Response

To maximize participation in the DR programs, a few fundamental questions should be addressed. What is the role of SO to facilitate the DR actions in the market? What changes are recommended in the market rules and regulations that will influence consumer behavior in DR? A primary challenge to promote DR is the technological barrier. Enabling the smart technologies and advanced metering infrastructure would allow the consumers to access timely information and automate their load responses. In recent years, aggregator or community load controller guided DR programs have gained attention. Aggregators represent interests of large groups of consumers

in smart & connected communities by monitoring prices, scheduling loads, and sharing stored energy to minimize cost. Another barrier that prevents the DR action is pricing practices. Current pricing structure in most of the electricity markets is flat (unit price of electricity is constant throughout the year). A flat price does not reflect the varying wholesale prices. At present, very few markets follow real-time pricing, where consumer are informed of a wholesale prices at the end of each hour. In both flat and real-time pricing approaches, the SO or utilities have failed to attract the consumers to engage in DR actions. A true DR can only be accomplished if SO offers advance price signals to the consumers.

1.1.5 Pricing Practices in Power Markets

Pricing is a key stimulus for DR actions. In other words, DR cannot be implemented effectively if SO fails to select an appropriate pricing design in the market. There exist widely varying electricity tariff structures. It ranges from fixing a rate one year in advance to sending price signals right before the dispatch. The amount of risk and reward to the consumers are considered in determining these pricing schemes [8]. Time of use (TOU) [9] and critical peak pricing (CPP) [10] are the traditional pricing practices to involve consumers in the demand response program. The major drawback in these practices is that they do not reflect the wholesale market prices and fail to capture the market operating conditions. At present, real-time pricing (RTP) schemes are used in limited markets (Ameron [11] and ComED [12]) to involve the residential user in demand response practice. Though RTP scheme is dynamic, it reveals the prices to the consumers after the consumption is done. This puts the consumer in a financial risk against the flat price. The most desirable pricing practice to maximize the DR potential would be disclosing the price of electricity before consumption (dynamic pricing), currently this practice is not available in any power markets.

1.1.6 Challenges and Opportunities in Offering Dynamic Prices

The dynamic prices offered by SO should influence the consumer behavior and increase the awareness of energy consumption. Furthermore, it should reflect or closely follow the wholesale market. The price signal offered before consumption will help the consumers to alter their demand during high price peaks and vice-versa. As a consequence, SO might encounter financial risk in the market when their projected load differs from realized load. A proper understanding of the consumer behavior in a market is thus vital to develop a dynamic pricing strategy. If the dynamic prices and aggregators-guided DR strategies are not aligned properly through design, there may be greater peaks in demand than normal conditions. Hence, the dynamic prices and DR strategies should be designed carefully to reduce the network stress i.e., transmission flows.

1.2 The Problem Statement

The overarching problem examined in this dissertation is to demonstrate if it is viable to trade electricity like other commodities, where price is declared ahead of consumption and also allow the consumers to engage in DR actions. The dynamic pricing and DR decisions are based on the interactions between SO and the load aggregators. The true essence of dynamic pricing is to offer a monetary benefits to the consumers (guided by aggregators) for shifting their load consumption and balance the demand in electricity network. The aggregator enabled DR should guarantee a reduction in total cost of consumption by shifting the consumers' loads using consumers' preferences. The SO is responsible to decide, beforehand, how much price to charge the consumers during each hour of a day, such that any deviation of load pattern (due to DR actions) should not result in huge surpluses or deficits in revenue collected by the SO. The objectives of the game between the SO and the aggregator is therefore to minimize the revenue

loss incurred to the SO and minimize the billing charges to the consumers. The major assumption adopted in this problem is: aggregator guided DR improves users' rationale in the event of price changes. However, true aggregator behavior has not yet been fully investigated. It is also assumed that consumers submit their load characteristics and operating preference to the aggregator a day before the consumption. The broader issue is, as the SO delivers an advance binding price signal (say, an hour ahead) to the aggregators this provides planning time for aggregators to decide their consumption. If the price declared is not aligned with the prediction of aggregator usage and shifting behavior, then SO will be exposed to unacceptable financial risk. Furthermore, it also poses a threat to system reliability. As regards aggregators, the SO informs the binding price signal only for the current interval. Hence, the aggregators should forecast the binding prices of the future hours to determine the energy usage for the current time interval and the future time intervals. The overall objective is to design stable and coordinated strategies for dynamic pricing and demand response in power network.

1.3 Research Contributions

The detailed description of research contributions are presented in the subsequent chapters. In what follows, an overview of the research contributions and the broader impacts are presented.

1.3.1 Data-driven Agent-based Learning Model

With the growth of internet of things and AMI, the consumers will increasingly be able to alter their consumption patterns based on the knowledge of hourly price variations.

Per current practice, the SO uses/estimates hourly DA demand and procures those quantity in the DA market for DA price. If the consumers do not alter their actual consumption from the DA quantity, then the DA price as a dynamic price works well and this also keeps the SO in revenue neutral status.

However, with the aggregators' ability to shift and adjust consumption, if the DA price is offered as a dynamic price, then the aggregators can switch their loads to lower price periods for monetary benefits. This will force the SO to curtail production in hours of reduced consumption while procuring more from the real time market (generally more expensive) during hours where loads are shifted. This will make the revenue earned by SOs less than the pay-out to the generators. Hence, in the presence of load switching ability, SO needs to find an appropriate pricing strategy (not the DA prices) that will encourage DR while not incurring revenue loss. To achieve this, a closed-loop comprehensive methodology guided by a data-driven learning model is developed. The methodology is implemented on a sample network. It is shown that such a methodology can yield stable and coordinated strategies for SO to offer dynamic prices as well as for aggregators to take DR actions for the consumers. The dynamic pricing decision is primarily influenced by supply bids in the DA and RT markets, expected DR actions, and network congestion. For the given dynamic prices offered by the SO, the aggregators' DR actions are obtained from a robust optimization model. Hence, the methodology is a simulation-optimization based approach that learns both dynamic prices and DR actions. These strategies keep the SO revenue neutral and at the same time reduce the cost of consumption to the consumers. A significant added benefit that the methodology offers is an improved load balance in the network. Sensitivity analysis shows that increase in the percentage of deferrable loads would yield higher financial benefits for the consumers, since DR lowers the daily average price of electricity.

1.3.2 Game-theoretical Model

In the data-driven model, the DR is provided by residential and business appliances with the support of AMI and IoT platforms. One of the key contribution in this game-theoretical model is, a large volume of EVs take part in DR actions, and all residential and/or business loads in the

network are remain fixed. Since, we believe that the forthcoming growth of EVs will provide new opportunities through optimally scheduling the EV charging needs and it can be consider as a supplement to the traditional DR. So, a granular EV parking lot model is designed and it comprised of large volume of EVs with different makes and models, battery capacities and charging needs. This model focuses on interaction between the SO and aggregator managed EV parking lots, who decides the optimal charging strategies for the EVs based on the hourly dynamic price offered by the SO.

A two-layer model is developed for the DA and RT market operations, where the top-layer uses a two-stage stochastic model that addresses the DA operations and bottom layer adopts bilevel structure for the real-time interaction between the SO and aggregators. Price spikes are considered inherent in the network, which causes real-time price uncertainties. These uncertainties are accommodated in the bilevel model using a robust optimization framework. Hence, the problem exhibits a robust bilevel structure, where SO determines the hourly dynamic price schedule by ensuring revenue neutral status (upper-level problem), and the aggregators decide the corresponding optimal charging schedules of EVs (DR strategies). The aggregators' aim is to lower the daily average consumer cost in the network that are subjected to price spikes. Furthermore, a granular EV parking lot model is designed and it comprises of large volume of EVs with different makes and models, battery capacities and charging needs.

1.4 Broader Impacts

In the new millennium, a revolutionary change has begun in the power networks, where supply following the demand is transformed into demand following the supply. This is referred to as demand response. To facilitate the DR actions among consumers, policy makers have implemented various limited forms of dynamic pricing to benefit both SO and the consumers. The

most desirable form of dynamic pricing is ex-ante real-time pricing, where the consumers are offered prices ahead of consumption. Literature reported major concerns from the practitioners and researchers that if the ex-ante dynamic pricing and the corresponding DR strategies are not aligned properly, there may be higher demand peaks than normally experienced, and this will results in higher price spikes and thus may instigate worst outcomes like blackouts. Stable policies for (ex-ante) dynamic pricing and corresponding DR strategies that are developed using the granular methodology presented in this dissertation helps to dispel the above concern.

Our research also establishes that a pure form of dynamic pricing is a key enabler for DR actions. Dynamic pricing along with technology (IoT and AMI) can greatly improve consumer participation, yielding cost reduction benefits to the consumers and reduction of the network overload via better load balance.

It is established in this dissertation that the growth of EVs offers a unique opportunity for increased DR in the future, as the EV charging can be scheduled optimally take advantage of low peak periods. A granular model for EV integration through smart parking lots under dynamic pricing is a novel contribution of this dissertation.

It is shown that the proposed dynamic pricing policy performs better compared to all other existing limited forms of dynamic pricing in power networks.

1.5 Summary of Dissertation

Proliferation of AMI and the practice of disclosing the price of electricity before consumption (dynamic pricing) are the two key enablers for demand response reaching its full potential. With increasing deployment of AMI and aggregator managed demand response narrows the technology gaps. So, the spotlight is on dynamic pricing. In Chapter 2, a comprehensive closed-loop data-driven methodology is presented to design stable and coordinated strategies for dynamic

pricing and demand response. The methodology uses Bayesian load prediction model to update the DA quantity, and the SO with the support of optimal power flow formulation determines the DA prices. Thereafter, SO uses a learning model to obtain hourly dynamic prices for the each hour of the next day. At each iteration, variation in dynamic price allows the aggregators to gradually alter their DR pattern. This process, when continued for many iterations, yield a suitable dynamic pricing strategy and a corresponding DR actions for the aggregators. The stable strategies derived from this methodology implemented on a congested network show that it is possible to achieve a significant reduction in price of electricity and improve network load balance which in turn reduces the need for expensive (most idle) reserve generation capacity. This is an offline simulation tool that allows both SO and aggregator to learn stable policies without affecting both the network and market operations during the learning process.

An alternative to DR by business and residential consumer appliances, which needs a widespread availability of IoT and AMI, is the EV parking lots that will host large numbers of EVs that can significantly contribute for DR. These EV parking lots will benefit from dynamic pricing by inducing increased DR. A robust game-theoretical model is presented in Chapter 3, where the interaction between the SO and EV parking lots determine the dynamic pricing strategy for SO and optimal charging needs (demand response) for EV parking lots. The SO determines the dynamic pricing by considering the financial settlement in both DA and RT market. A two-layer model is formulated where the top-layer (a two-stage stochastic model) addresses the day-ahead schedule, and the bottom-layer (a bilevel model) obtains the real-time decisions comprising dynamic prices and optimal charging schedule for EVs on an hourly basis. The bilevel model also accommodates the real-time price uncertainties (price spikes) using a robust optimization approach. Numerical results show dynamic pricing as superior to prevailing pricing policies.

In Chapter 4, a controlled islanding of power networks anticipating severity of extreme events is proposed. It is evident that rapid climate change will continue to cause severe events with greater disruptions to the power networks. It is important to develop better means of avoiding system wide failures and to make the grid more resilient. Hence, controlled islanding is essential to harden power networks against widespread outages caused by extreme weather events. Planned islanding approaches can optimally utilize generating and other resources to minimize load shedding in the grid. A graph theoretical approach with mixed integer programming formulation is presented to minimize the total cost of islanding.

CHAPTER 2: A DATA-DRIVEN METHODOLOGY FOR DYNAMIC PRICING AND DEMAND RESPONSE IN ELECTRIC POWER NETWORKS

The complete article on *A Data-Driven Methodology for Dynamic Pricing and Demand Response in Electric Power Networks* (submitted to Electric Power Systems Research Journal) can be found in Appendix C. This article presents a comprehensive data-driven methodology that can simultaneously yield stable and coordinated policies for dynamic pricing and corresponding demand response actions in a smart and connected communities.

2.1 Abstract

The practice of disclosing price of electricity before consumption (dynamic pricing) is essential to promote aggregator-based demand response in smart and connected communities. However, both practitioners and researchers have expressed the fear that wild fluctuations in demand response resulting from dynamic pricing may adversely affect the stability of both the network and the market. This paper presents a comprehensive methodology guided by a data-driven learning model to develop stable and coordinated strategies for both dynamic pricing as well as demand response. The methodology is designed to learn offline without interfering with network operations. Application of the methodology is demonstrated using a sample 5-bus PJM network. Results show that it is possible to arrive at stable dynamic pricing and demand response strategies that can reduce price of electricity as well as improve network load balance.

CHAPTER 3: A TWO-LAYER MODEL FOR DYNAMIC PRICING OF ELECTRICITY AND OPTIMAL CHARGING OF ELECTRIC VEHICLES UNDER PRICE SPIKES

The complete article on *A Two-Layer Model for Dynamic Pricing of Electricity and Optimal Charging of Electric Vehicles under Price Spikes* [13] (published in Energy Journal) can be found in Appendix D. This article presents a two-layer optimization model that can simultaneously yield dynamic pricing policy for SO and corresponding demand response strategies for EV parking lots.

3.1 Abstract

Pilot projects in power networks conducted across continents have established the benefits of dynamic pricing by inducing increased demand response. However, a key hurdle in the growth of demand response is the lack of widespread availability of advanced metering infrastructure, which has stymied the adoption of dynamic pricing. We believe that this hurdle will be partially addressed by the growth of electric vehicles (EVs), as smart and connected EV parking lots will be a provider of demand response. We develop a two-layer optimization model that simultaneously determines dynamic pricing policy for the system operator and demand response strategies for the EV parking lots. The model minimizes the cost to consumers, while ensuring the system operator's revenue neutral status and addressing real-time price uncertainties. A variant of the 5-bus PJM network is used to demonstrate model implementation. Numerical results show that for a low to moderate price spike scenario, dynamic pricing with demand response from EVs alone can lower the daily average consumer cost of 1.42% compared to the cost of at pricing. A cost reduction of

6.5% is achieved when price spikes are relatively high. Computational challenges of implementing our model for real networks are discussed in the concluding remarks.

3.2 Electric Vehicles on Power Networks

In electricity network, it is observed that elasticity of demand is deemed important to overcome wild fluctuations concerning both energy market and network operations. The growing demand and increased penetration of intermittent energy resources are the two primary factors responsible for this wild fluctuations. As anticipated, we are close to the tipping point where high volume of EVs hitting the road are inevitable and a huge challenge is awaiting for the power networks to integrate EV parking lots into the grid. Despite the huge forecasted demand growth, a lot more demand elasticity is achievable if the EVs in parking lots are charged in smart and coordinated approach, and that could offer a greater benefit to the grid. It is important to utilize their flexible operation characteristics and pictured them as a grid asset under uncertain environment.

3.2.1 Challenges and Opportunities

Deployment of large volume of EVs in the grid will induce a significant impact in both network design and operations [14]. As these loads are more dynamic in nature, smart meters and timely communication infrastructure [15] are critically needed to promote pricing framework and also to create a favorable environment for smart charging approach. It was reported in [16], smart charging strategies could evade 60 - 70 % of incremental investment in distribution networks. In [17], AMI with dynamic pricing are considered as an effective tool to obtain optimal EV charging schedule. Further, it was found out through an experiment that there is a 36% reduction in peak consumption. EV parking lots can act as a both consumer and energy producer. A framework has been proposed in [18] to integrate batteries of EV into grid as a distributed energy resources. The

system operator coordinating with aggregated EVs could increase the efficiency and security of both the electricity networks and the power markets [19]. In few markets, the EV parking lots can participate in day-ahead energy bidding and also in reserve markets. The bidding strategies of EV parking lots have proposed and investigated in [20]. In addition to vehicle to grid energy injection, EV can transfer energy to homes (V2H) [21] and also to buildings (V2B) [22] to reduce their demand peaks.

CHAPTER 4: CONTROLLED ISLANDING OF POWER NETWORKS BASED ON ANTICIPATED SEVERITY OF EXTREME EVENTS

The complete article on *Controlled Islanding of Power Networks based on Anticipated Severity of Extreme Events* [23] (published in IEEE Power & Energy Society General Meeting 2018) can be found in Appendix E. This article presents a graph theoretical mixed integer programming model to develop controlled islanding strategies for power network anticipating severity of extreme events.

4.1 Abstract

A new mixed integer programming model is presented for developing islanding strategies for power grids when disruptions from extreme events are anticipated. It minimizes the total cost arising from planned load reduction together with the cost of unplanned load loss and network recovery. The later cost is a function of the severity of the anticipated extreme event. The model selects an appropriate number of islands and their sizes depending on the severity, islanding results for IEEE 30-bus and 29-bus GB test system is presented. The MIP model considers anticipated severity of the event related parameter α as an input, which has not been considered earlier. We demonstrate via the IEEE 30-bus network that if a high value of upper bound for the number of islands is chosen, the model determines the appropriate number of islands based on the severity.

CHAPTER 5: CONCLUSIONS

A pure form of dynamic pricing and demand response (DR) can be considered as an effective mechanism to improve functioning of power system operations. Fast deployment of AMI will create a new opportunities in DR by delivering direct economic gains for the consumers. In addition to that, proliferation of EV will offer a new dimension to DR by shifting EV battery charging needs and manage them flexibly to support the grid operations. It has been argued that implementation of full-fledged DR requires a favorable regulatory reforms [24] and proper pricing practices [7]. True DR will need to be supplemented by appropriate dynamic pricing policies by the SO. The key features of such policies should include 1) the binding dynamic prices are declared in advance of consumer usage, and 2) the declared prices should not deviate appreciably from the market price resulting from DR actions. The first feature will promote more DR and also lowers the cost of electricity. The latter feature ensures the SO revenue collected from the consumers is close to the amount paid to the producers. The latter feature also needs a proper understanding of aggregator (collective consumer) behavior in a market. Hence, the dynamic pricing by SO and corresponding aggregator-guided DR strategies should aligned properly through design to avoid greater peaks in demand.

A comprehensive agent-based methodology that uses data-driven learning models are developed to support policy makers (SO and aggregators), through repetitive interactions, to learn each other behavior and to yield a stable and coordinated strategies for dynamic pricing and corresponding DR actions. The complete description on the methodology is presented in chapter

2 and appendix. Numerical results on a sample network shows that the SO and aggregator can learn their strategies through an offline simulation models and that obtains a stable policies for dynamic pricing and DR, respectively, without disrupting actual network operations. Two key observations are made from the results, 1) such polices can reduce the price of electricity paid by the consumers through increased load balance, and 2) SO, being a non-profit agent, can offer dynamic prices without accumulating surplus revenue or shortfall.

To supplement the lack of widespread availability of AMI, smart and connected EV parking lots are adopted for DR. In chapter 3 and appendix, a two-layer optimization model is developed that simultaneously yield dynamic pricing policy for SO and optimal charging (demand response) strategies for aggregator guided EV parking lots. In the two-layer model, the top layer (two-stage stochastic model) addresses the day-ahead schedule and the bottom-layer (a bilevel model) obtains the real-time decisions. Numerical implementation on a sample network shows that the daily average consumer cost is reduced by 1.5% when the consumers adopted dynamic pricing and demand response. It also evident that dynamic pricing policies obtained in this model as superior to other prevailing pricing policies in the market.

The interconnected power networks are more vulnerable to cascading failure in the event of extreme events. This leads to a major disruption and unable to serve the consumers. A planned islanding strategy is developed using graph-theoretical model that determines an optimal level of islanding considering anticipated severity of extreme events. The model is implemented on IEEE 30 bus system and 29-bus GB network, the model determines the appropriate number of islanding needed based on the severity levels.

REFERENCES

[1] C. Andrews and S. Govil, "Becoming proactive about environmental risks: regulatory reform and risk management in the US electricity sector," Energy Policy, vol. 23, no. 10, pp. 885-892, 1995.

[2] A. Faruqui, R. Hledik, S. Newell and Pfeifenberger, "The power of 5 percent," The Electricity Journal, vol. 20, no. 8, pp. pp.68-77, 2007.

[3] S. Borenstein, M. Jaske and A. Rosenfeld, "Dynamic pricing, advanced metering, and demand response in," Center for the Study of Energy Markets, UC Berkeley, 2002.

[4] A. Faruqui, A. Hajos, R. Hledik and S. and Newell, "Fostering economic demand response in the Midwest ISO," Energy, vol. 35, no. 4, pp. pp. 1544-1552, 2010.

[5] L. Wenpeng, "Advanced metering infrastructure.," Southern Power System Technology, vol. 3, no. 2, pp. pp.6-10, 2009.

[6] B. Shen, G. Ghatikar, Z. Lei, J. Li, G. Wikler and P. and Martin, "The role of regulatory reforms, market changes, and technology development to make demand response a viable resource in meeting energy challenges," Applied Energy, vol. 130, pp. pp. 814-823, 2014.

[7] S. Borenstein, "Time-varying retail electricity prices: Theory and practice.," in Electricity degulation: choices and challenges, Chicago, The university of Chicago, 2005, pp. pp. 317-356.

[8] A. a. P. J. Faruqui, "Dynamic pricing and its discontents," Regulation, vol. 34, pp. pp. 16-23, 2011.

[9] M. Filippini, "Electricity demand by time of use an application of the household aids model," Energy Economics, vol. 17, no. 3, pp. pp. 197-204, 1995.

[10] K. Herter and P. a. R. A. McAuli, "An exploratory analysis of California residential customer response to critical peak pricing of electricity," Energy, vol. 32, no. 1, pp. pp. 25-34, 2007.

[11] "Real time pricing," Elevate Energy, [Online]. Available: http://www.elevateenergy.org/blog. [Accessed 25 July 2017].

[12] "Real time pricing," Comed, 2015. [Online]. Available: ttps://www.comed.com/Pages/default.aspx. [Accessed 25 July 2017].

[13] Subramanian, Vignesh, and Tapas K. Das. "A two-layer model for dynamic pricing of electricity and optimal charging of electric vehicles under price spikes." Energy 167 (2019): 1266-1277.

[14] J. Lopes, F. Soares and P. and Almeida, "Integration of electric vehicles in the electric power system," Proceedings of the IEEE, vol. 99, no. 1, pp. pp. 168-183, 2011.

[15] V. Gungor, D. Sahin, T. Kocak, S. Ergut, C. Buccella, C. Cecati and G. and Hancke, "A survey on smart grid potential applications and communication requirements," IEEE Transactions on industrial informatics, vol. 9, no. 1, pp. pp. 28-42, 2013.

[16] L. Fernandez, T. San Romn, R. Cossent, C. Domingo and P. and Frias, "Assessment of the impact of plug-in electric vehicles on distribution networks," IEEE transactions on power systems, vol. 26, no. 1, pp. pp. 206-213, 2011.

[17] L. Lam, K. Ko, H. Tung, H. Tung, W. Lee, K. Tsang and L. and Lai, "Advanced metering infrastructure for electric vehicle charging," Smart Grid and Renewable Energy, vol. 2, no. 4, p. pp. 312, 2011.

[18] C. Guille and G. and Gross, "A conceptual framework for the vehicle-to-grid (V2G) implementation," Energy policy, vol. 37, no. 11, pp. pp. 4379-4390, 2009.

[19] M. Ortega-Vazquez, F. Bouffard and V. and Silva, "Electric vehicle aggregator/system operator coordination for charging scheduling and service procurement," IEEE Transaction on Power Systems, vol. 28, no. 2, pp. pp.1806-1815, 2013.

[20] R. Bessa, M. Matos, F. Soares and J. and Lopes, "Optimized bidding of a EV aggregation agent in the electricity market," IEEE Transactions on Smart Grid, vol. 3, no. 1, pp. pp. 443-452, 2012.

[21] A. Dargahi, S. Ploix, A. Soroudi and F. and Wurtz, "Optimal household energy management using V2H flexibilities," The International Journal for Computation and Mathematics in Electrical and Electronic Engineering, vol. 33, no. 3, pp. pp. 777-792, 2014.

[22] C. Marmaras, M. Corsaro, E. Xydas, L. Cipcigan and M. and Pastorelli, "Vehicle-to-building control approach for EV charging," in In Power Engineering Conference (UPEC), 2014 49th International Universities (pp. 1-6). IEEE, 2014.

[23] Vignesh Subramanian, Tapas K. Das, and Hadi Charkhgard, "Controlled Islanding of Power Networks Based on Anticipated Severity of Extreme Events", IEEE Power & Energy Society General Meeting (PESGM, 2018.

[24] B. Shen, G. Ghatikar, Z. Lei, J. Li, G. Wikler and P. Martin, "The role of regulatory reforms, market changes, and technology development to make demand response a viable resource in meeting energy challenges," Applied Energy, vol. 130, pp. 814-823, 2014.

APPENDICES

Appendix A: General Information about Appendices

Appendices include the copyright authorizations for the published material in the journal of Energy and IEEE Power & Energy General Meeting

Appendix B: Copyrights for Published Materials in Energy Journal

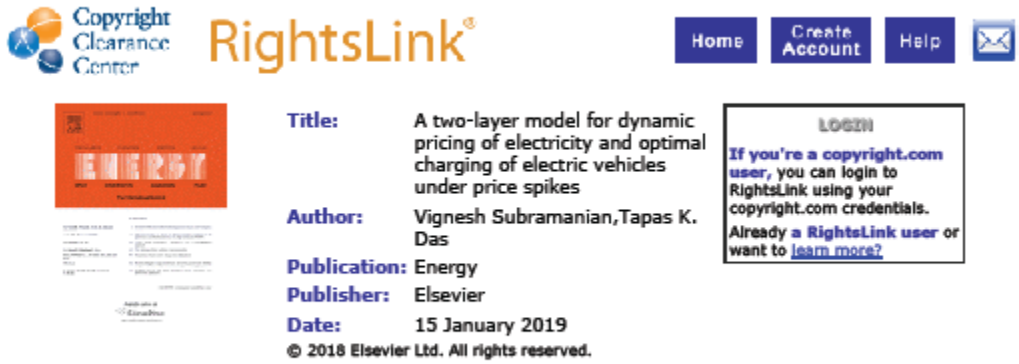

Copyright Clearance Center RightsLink®

Home | Create Account | Help

Title: A two-layer model for dynamic pricing of electricity and optimal charging of electric vehicles under price spikes

Author: Vignesh Subramanian,Tapas K. Das

Publication: Energy

Publisher: Elsevier

Date: 15 January 2019

LOGIN

If you're a copyright.com user, you can login to RightsLink using your copyright.com credentials.

Already a RightsLink user or want to learn more?

Please note that, as the author of this Elsevier article, you retain the right to include it in a thesis or dissertation, provided it is not published commercially. Permission is not required, but please ensure that you reference the journal as the original source. For more information on this and on your other retained rights, please visit: https://www.elsevier.com/about/our-business/policies/copyright#Author-rights

BACK CLOSE WINDOW

Appendix C: Article Submitted in Electric Power Systems Research Journal

A Data-Driven Methodology for Dynamic Pricing and Demand Response in Electric Power Networks

Vignesh Subramanian[a,*], Tapas K. Das[a], Changhyun Kwon[a], Abhijit Gosavi[b]

[a] *Department of Industrial and Management Systems Engineering, University of South Florida, Tampa, FL, 33620 USA*

[b] *Department of Engineering Management & Systems Engineering, Missouri University of Science and Technology, Rolla, MO, 65409 USA*

Abstract

The practice of disclosing price of electricity before consumption (dynamic pricing) is essential to promote aggregator-based demand response in smart and connected communities. However, both practitioners and researchers have expressed the fear that wild fluctuations in demand response resulting from dynamic pricing may adversely affect the stability of both the network and the market. This paper presents a comprehensive methodology guided by a data-driven learning model to develop stable and coordinated strategies for both dynamic pricing as well as demand response. The methodology is designed to learn offline without interfering with network operations. Application of the methodology is demonstrated using a sample 5-bus PJM network. Results show that it is possible to arrive at stable dynamic pricing and demand response strategies that can reduce price of electricity as well as improve network load balance.

Keywords: Dynamic pricing, aggregated demand response, electric power network, Bayesian demand prediction.

*Corresponding author

Email address: vigneshs@mail.usf.edu (Vignesh Subramanian)

1. Introduction

Grid modernization will continue to enhance timely communication among the system operator (SO), producers, and load aggregators. This will provide the infrastructure to implement dynamic pricing of electricity and increase demand response (DR) participation. The phrase *dynamic pricing* has various interpretations in practice and is used to refer to policies like critical peak pricing, real-time pricing and many variants thereof. In this paper, the term *dynamic pricing* is used to refer to the practice of offering binding price of electricity just ahead of consumption. Whereas, the term DR will refer to the load scheduling action by aggregators based on price of electricity and preferences of the consumers in the households, businesses, and industries. DR has long been recognized as an effective mechanism to improve functioning of power network operation. Implementation of full fledged DR programs will require appropriate pricing practices [1]. Dynamic pricing has been identified as a key to promote DR, early in the millennium [2] and more recently [3, 4]. However, till date, dynamic pricing policies have remained limited in the U.S. to time of use (TOU) pricing, critical peak pricing (CPP), ex-post real time pricing (RTP), among others. Many pilot projects across three continents in recent years have examined the benefits of dynamic pricing on load balancing and consumer cost reduction [5, 6, 7].

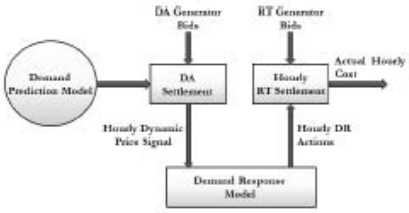

Fig. 1. Dynamic pricing and DR framework

In this paper, we develop a comprehensive methodology to design complimentary policies for dynamic pricing decision by the system operator and the DR actions by the load aggregators, while considering both market and network characteristics. The framework of our methodology is depicted in Fig. 1. The load aggregators predict the day-ahead (DA) hourly demand by applying a Bayesian model

on historical demand data (prior) and the most recent hourly demand (based on DR actions). It is assumed that the load aggregators are price takers and submit the predicted DA quantities as demand bids to the system operator (SO). Using these demand bids and the DA price bids submitted by the generators, the SO obtains a DA schedule through a network constrained least cost dispatch approach. This yields DA hourly quantities and corresponding LMPs. Now, before each hour of actual dispatch, the SO determines the binding nodal dynamic prices and offers those to the aggregators. The SO obtains these dynamic prices using an exponential learning model with two inputs: the DA price and the previous day's dynamic price for the current hour. The aggregators at the load nodes decide their DR actions (consumption plan) for the current and the remaining hours of the day using the binding dynamic prices for the current hour and the predicted dynamic prices for the future hours, which they obtain using a regression model. Any deviation in load consumption for the current hour from the DA demand bid is settled using the real-time (RT) prices. It is considered that the generators submit separate RT bids to the SO, and the SO settles the market to pay the generators for the hour using a two-settlement (DA and RT) approach. This determines the cost to the SO for satisfying the demands. Note that, the SO's revenue depends on the binding dynamic prices and the correponding DR decisions by the aggregators, which in turn determines the cost to the SO. Hence, if the dynamic prices are not designed properly, the resulting DR actions may lead to imbalance in the revenue and cost for the SO. Our model is designed to obtain stable dynamic pricing and demand response policies to improve load balance and reduce cost to the consumers, while maintaining revenue neutral status of the SO. A recent paper [8] addresses a similar problem using a closed loop dynamical system model and derives stable ex-ante pricing strategy for each interval of a network operation and the corresponding DR strategies. Our methodology offers a data-driven learning approach that is granular and can consider different

types of load, their operating preferences, network constraints, and a two-settlement approach for the market.

Literature shows that availability of smart technology (eg., advanced metering infrastructure, AMI) increases price elasticity and grid efficiency [9, 10]. Beneficial impacts of dynamic pricing have been explored via seventy-four pricing experiments across three continents during the last decade [5]. The results in these studies show that in the presence of higher price peaks better benefits of load balancing from dynamic pricing. It is shown in [7] that dynamic pricing can achieve a peak demand reduction of 10-14%, customer cost reduction of 2-5%, and a social welfare increase by \$141-\$403 million in a year. A study conducted in California [6] found that most consumers will benefit from dynamic pricing, and also that low income consumers will not be impacted negatively, a concern that was expressed earlier. The study presented in [11] claimed that a careful design of dynamic pricing schemes is needed to increase the consumer flexibility. A balanced RTP strategy was proposed in [12] where the consumers are offered binding prices ahead of consumption (ex-ante prices). Need to understand consumer behavior in a market to address volatility between the ex-ante and ex-post prices, inherent in networks with RTP and DR, is emphasized in [13]. It was argued in [14, 15] that if the RTP and the corresponding aggregator-guided DR strategies are not aligned properly through design, there may be greater peaks in demand than normal condition, which might instigate worst outcomes like blackouts.

As reported in [2], even a slight DR participation may significantly reduce the wholesale electricity prices. It is claimed that DR assisted balancing of consumer demand and resulting increase in load factor will ease the burden of current practice of maintaining peaking generation capacity at the level of 10 - 15% of the expected demand [16]. In recent years, aggregator-guided DR has been proposed [17]. Aggregators represent interests of large groups of consumers (households, factories, and businesses) by

monitoring and scheduling loads to minimize cost. With emerging home and building energy management systems [18, 19], even individual consumers are being empowered to engage in DR. Proliferation of smart grid with smart appliances will continue to extend the potential of DR [20]. Aggregator-guided DR is claimed to improve users' rationale in the event of price changes, however, true aggregator behavior is yet to be investigated [21]; the authors present an iterative approach to design real time pricing algorithms to minimize the peak-to-average demand ratio. Other approaches adopted for aggregator coordinated DR can be found in [22, 23]. A dynamic energy management framework to simulate DR and to estimate consumer behavior is proposed in [24]. Similar work with minimization of electricity price as a DR objective, can be found in [25, 26]. To our knowledge, most of openly available methods for real time pricing and DR are developed using limited history of price and consumption data. Some of the recent pilot studies that model data to demonstrate potential DR benefits are [27, 28].

The remainder of this paper is organized as follows. The complete methodology is described in Section 2. Section 3 contains a numerical demonstration of the methodology on a modified 5-bus PJM network. Concluding remarks are offered in section 4.

2. Dynamic pricing & DR Methodology

Fig. 2 shows the model elements of the dynamic pricing & DR methodology. In what follows, we provide details of each model.

2.1. Bayesian DA demand prediction model

The aggregator at each load node submit their fixed hourly DA demand bids to SO, which are predicted using the model given here. Let K denote the number of nodes (or buses) in the network. At any node $k \in \{1, \cdots, K\}$ and hour $t \in \{1, \cdots, 24\}$, let $x_{1,(k,t)}, x_{2,(k,t)}, \cdots, x_{n,(k,t)}$ denote the historical hourly load data for the demand random

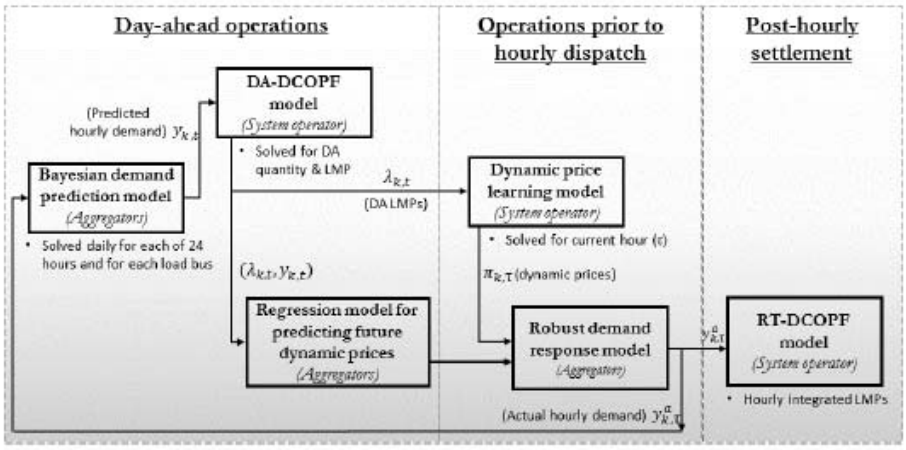

Fig. 2. Elements of dynamic pricing and DR methodology

variable $X_{k,t}$. We assume that this data is characterized by a normal distribution $N(\mu_{k,t}, \sigma^2_{k,t})$, which is thus the prior $f(x_{k,t})$ for the demand $X_{k,t}$.

Let, for each hour of a day, the aggregator's DR action yields an actual demand denoted by $y^a_{k,t}$. Then we can write the random variable for the actual demand generated by DR action $Y^a_{k,t}$ as $Y^a_{k,t}|\left(X_{k,t} = x_{k,t}\right) \sim N\left(x_{k,t}, \sigma^2_{k,t}\right)$. We assume that the variance of the demand resulting from DR action is same as that of the prior. Hence, the likelihood for the observed data $y^a_{k,t}$ can be written as

$$L(x_{k,t}|y^a_{k,t}) = f(y^a_{k,t}|x_{k,t}) = (2\pi\sigma^2_{k,t})^{-1/2} \exp \frac{-1}{2\sigma^2_{k,t}}(y^a_{k,t} - x_{k,t})^2 \quad \forall t \in \{1, \cdots, 24\}, \forall k \in \{1, \cdots, K\}. \tag{1}$$

Using Bayes' theorem, the posterior distribution (which is proportional to the likelihood times the prior) can be written as,

$$f(x_{k,t}|y^a_{k,t}) \propto f(y^a_{k,t}|x_{k,t}).f(x_{k,t}) \propto \exp \frac{-1}{2\sigma^2_{k,t}}(y^a_{k,t} - x_{k,t})^2 \cdot \exp \frac{-1}{2\sigma^2_{k,t}}(x_{k,t} - \mu_{k,t})^2. \tag{2}$$

The posterior distribution of the normal conjugate prior is also a normal distribution, the mean of which can be written as $E\left[X_{k,t}|y^a_{k,t}\right] = \arg\max_{x_{k,t}} \ln f(x_{k,t}|y^a_{k,t})$. The posterior mean can then be obtained, by equating to zero the first order partial derivative

of the log-likelihood of $f(x_{k,t}|y^a_{k,t})$ with respect to $x_{k,t}$, as follows:

$$\frac{\partial \ln f(x_{k,t}|y^a_{k,t})}{\partial x_{k,t}} = \frac{1}{\sigma^2_{k,t}}(y^a_{k,t} - x_{k,t}) + \frac{-1}{\sigma^2_{k,t}}(x_{k,t} - \mu_{k,t}) = 0. \tag{3}$$

The above yields $E\left[X_{k,t}|y^a_{k,t}\right] = \frac{y^a_{k,t}+\mu_{k,t}}{2}$. Variance of the posterior distribution $\text{Var}(X_{k,t}|y^a_{k,t})$ is inverse of the Fisher information $I(X_{k,t}|y^a_{k,t})$, which is obtained as,

$$I(X_{k,t}|y^a_{k,t}) = -E\left[\frac{\partial^2 \log f(x_{k,t}|y^a_{k,t})}{\partial x^2_{k,t}}\right] = -\left(-\frac{1}{\sigma^2_{k,t}} - \frac{1}{\sigma^2_{k,t}}\right) = \frac{2}{\sigma^2_{k,t}}. \tag{4}$$

Hence, the posterior distribution is $N\left(\frac{\mu_{k,t}+y^a_{k,t}}{2}, \frac{\sigma^2_{k,t}}{2}\right)$. The mean hourly DA predicted demand vector for any node k is given by $\boldsymbol{y_k} = \left(\frac{\mu_{k,1}+y^a_{k,1}}{2}, \frac{\mu_{k,2}+y^a_{k,2}}{2}, \ldots, \frac{\mu_{k,24}+y^a_{k,24}}{2}\right)$. At the end of each day, the hourly actual demands resulting from the DR actions are added to the historical load data and are used to obtain new prior distribution parameters $(\mu_{k,t}, \sigma^2_{k,t})$ for the next day. Essentially, the aggregators update their prediction model for the next day based on their DR actions today.

2.2. Day-ahead settlement model

Based on the generators' DA supply offers $(C(P_{kt}))$ and the aggregators' DA demand bids $(y_{k,t})$, the SO solves a network constrained least cost dispatch model to obtain the locational marginal prices (LMPs) for each node at every hour of the following day. Let G_k represent the set of generators at node k. We assume that the generators' supply offer constitute quadratic functions given as $C(P_{kt}) = a_{kt}P^2_{kt} + b_{kt}P_{kt}$, $\forall i \in G_k, \forall k \in \{1, \cdots, K\}$, where P_{kt} is real power output supplied at node k by generator i . The DA settlement problem is formulated as a DCOPF [29] that minimizes the cost of supply offers, while meeting the supply-demand balance and other network constraints.

$$\min \sum_{k=1}^{K} \sum_{i \in G_k} a_{kt}P^2_{kt} + b_{kt}P_{kt}. \tag{5}$$

The dual variables from the power balance and the line flow constraints are decomposed into three components namely, marginal cost of energy at reference buses, marginal cost of losses, and the cost of congestion [30]. Using these, the LMPs $(\boldsymbol{\lambda_k})$ for all nodes are calculated. Solution of DCOPF for each hour yields $\boldsymbol{\lambda_k} = \{\lambda_{k,t}\}$, the set

of hourly DA LMPs for each node.

2.3. Regression model for predicting dynamic prices

The DR actions for each hour taken by the aggregators use the binding dynamic prices for the current hour and the predicted dynamic prices for the remaining hours of the day, which they obtain using the regression model. A piecewise linear regression equation is developed for each load node k with hourly demand as the independent variable and the corresponding cost (demand $\times$ DA price) as the dependent variable. We use a data set containing the current DA hourly demand-price pairs (D_k) and historical DA hourly demand-price pairs (D_k^h) for a number of days (say, H) to build the regression model. Note that $D_k^h = \{(y_{k,t}^h, \lambda_{k,t}^h) : \ \forall h \in \{1, 2, \cdots, H\}, \forall t \in \{1, 2, \cdots, 24\}\}$ and $D_k = (y_{k,t}, \lambda_{k,t})$. Considering a m piecewise components for the regression model, we maximize a set of (up to m) affine functions by minimizing the least square. Let U denote the $(H + 1) \times 24$ demand-price pairs in the data set used in the regression model. Denoting each demand-price pair as (y_u, λ_u) for $u \in U$, we write the following model to optimize the affine functions.

$$\min_{\beta_0^t, \beta_1^t} \sum_{u \in U} \left[\max_{t=1,\ldots,m} (\beta_0^t + \beta_1^t y_u) - y_u \lambda_u \right]^2. \tag{6}$$

The solution of the above yields an optimal set of l affine functions ($l \leq m$) and the corresponding l non-overlapping partitions of U. For more details on this approach, see [31].

2.4. A learning model for hourly dynamic prices

The SO obtains the nodal dynamic prices for each hour of the day by applying a learning model (as in [32]) on the previous day's dynamic price and the DA price. Let $\pi_{k,t}$ denote the dynamic price offered for node k at hour t, and $\gamma > 0$ denote the learning rate. Then, using $\hat{t}$ to denote the same hour t on the previous day, we write that

$$\pi_{k,t} = \gamma \lambda_{k,t} + (1 - \gamma) \pi_{k,\hat{t}}. \tag{7}$$

2.5. A robust DR model

We first describe the types of loads that are managed by the aggregators. Loads are either non-deferrable (fixed loads) or deferrable (shiftable and shift-adjustable loads). Deferrable loads are managed by the aggregators based on user preferences. Load curtailment is not considered as an option for aggregators in this model.

Non-deferrable load: These loads are fixed and have specified operation times and energy consumption levels. Let C denote the set of load consuming entities (e.g., homes, businesses, and factories) managed by an aggregator. For $i \in C$, let F_i denote the set of fixed loads and for each $j \in F_i$, f_{ijt} denotes the energy consumed during hour t.

Deferrable load: A deferrable load is characterized by its power consumption level, total duration of operation, and the interval(s) of time when it can be scheduled. These loads are further classified as shiftable (that are operated with rated power and have flexible hours of operation) and shift-adjustable (for which the power consumption levels can be adjustable along with the hours of operation). We denote the set of shiftable loads for load consuming entity i by S_i. For load $j \in S_i$, the consumption level is s_{ij} and the length of operation is τ_{ij}. The time window within which the operation can be scheduled is $[\underline{T^s}_{ij}, \overline{T^s}_{ij}]$. Hence, if x_{ijt} denote a binary variable indicating on/off status of a shiftable load at time t, we can write the operating constraint as

$$\sum_{t=\underline{T^s}_{ij}}^{\overline{T^s}_{ij}} x_{ijt} = \tau_{ij}, \qquad \forall i, j. \tag{8}$$

The set of shift-adjustable loads for an entity $i \in C$ is A_i. The rated (maximum) power consumption per unit time of the individual loads $j \in A_i$ is a_{ij}, which can be lowered up to a prescribed threshold $\underline{a}_{ij}$. The feasible operating time window of load $j \in A_i$ is $[\underline{T}_{ij}, \overline{T}_{ij}]$. Let u_{ijt} be a binary variable indicating the on/off status of $j \in A_i$ at time t, and α_{ijt} be a continuous variable indicating the level of power consumption. Then we

can write that

$$\underline{a}_{ij} \leq \alpha_{ijt}\, a_{ij} \leq a_{ij}, \qquad \forall i, j, t. \tag{9}$$

Denoting the total energy required to complete operation as E_{ij} , we can write

$$\sum_{t=\underline{T}_{ij}}^{\overline{T}_{ij}} u_{ijt}\, \alpha_{ijt}\, a_{ij} = E_{ij}, \qquad \forall i, j. \tag{10}$$

Note the above constraint is bi-linear in $u_{ijt}\ \alpha_{ijt}$. We linearize (10) by incorporating u_{ijt} in (9). Hence, we have

$$u_{ijt}\, \underline{a}_{ij} \leq \alpha_{ijt}\, a_{ij} \leq u_{ijt}\, a_{ij}, \qquad \forall i, j, t, \tag{11}$$

$$\sum_{t=\underline{T}_{ij}}^{\overline{T}_{ij}} \alpha_{ijt}\, a_{ij} = E_{ij}, \qquad \forall i, j. \tag{12}$$

Hence the total load scheduled by the aggregator at time t can be written as

$$y_t^a = \sum_{i \in C} \left[\sum_{j \in F_i} f_{ijt} + \sum_{j \in S_i} s_{ij} x_{ijt} + \sum_{j \in A_i} \alpha_{ijt}\, a_{ij} \right].$$

The aggregator finds y_t^a by solving an optimization model, described below, at each node at the top of each hour. The model uses 24-hour day as the planning horizon. For the current hour τ, based on the binding dynamic price π_τ, an aggregator determines the actual energy consumption for the current hour (y_τ^a) and the planned consumption for the remaining hours $t \in \{\tau+1, \cdots, 24\}$. The model uses the predicted values of the dynamic prices for the remaining hours from the piecewise regression model presented in Section 2.3. We note that these predicted values could differ from the dynamic prices offered by SO in the remaining hours. Such price variations present a risk of ineffective load scheduling. To reduce the impact of this risk, we adopt a robust optimization approach.

Let $\pi_t^{\max}$ denote the chosen upper $100 \times (1-\alpha)\%$ confidence bound of the historical values of the dynamic price for each hour t. These bounds are revised each day by updating the data history. Let Γ denote the parameter (in percent) for the degree of robustness, where Γ is 0% when price variations are not considered for any of the remaining hours, and Γ is 100% when price variations are considered for all of the

remaining hours, which yields the most conservative solution. For example, $\Gamma = 80\%$ means that the model considers price variations for $0.8 \times [24 - \tau]$ of the remaining hours. The robust DR model is presented next. For notational simplicity, we write the regression parameters as β_0 and β_1 (without their piecewise index i).

$$\min \ \pi_\tau y_\tau^a + \sum_{t=\tau+1}^{24} (\beta_0 + \beta_1 y_t^a) + \max_{\substack{\sum z \le \Gamma, \\ 0 \le z \le 1}} \sum_{t=\tau+1}^{24} [\pi_t^{\max} y_t^a - (\beta_0 + \beta_1 y_t^a)]\, z. \tag{13}$$

By duality principle as described in [33], we can rewrite the objective function as

$$\min \ \pi_\tau y_\tau^a + \sum_{t=\tau+1}^{24} (\beta_0 + \beta_1 y_t^a) + z\Gamma + \sum_{t=\tau+1}^{24} \zeta_t, \tag{14}$$

s.t.,

$$\text{Constraints (8), (11), \& (12)}, \tag{15}$$

$$z + \zeta_t \ge \pi_t^{\max} y_t^a - (\beta_0 + \beta_1 y_t^a), \qquad \forall t \in \{\tau + 1, \cdots, 24\}, \tag{16}$$

$$\zeta_t \ge 0, \ y_t^a \ge 0, \qquad \forall t \in \{\tau + 1, \cdots, 24\}, \tag{17}$$

$$z \ge 0, \ y_\tau^a \ge 0. \tag{18}$$

In the above model, the numerical values of β_0^t and β_1^t for the decision variable y_t^a are obtained using minimizing piecewise linear cost functions formulation.

2.6. Real-time settlement model

Once the aggregators take DR actions, variation between the DA demand and the actual consumption is settled by the SO using the real-time price bids in the DCOPF model. This two-settlement process yields the integrated LMPs, which we refer to as settled price in the numerical implementation study. Note that, the total payment made by the SO to the generators could be different from the total revenue collected from the aggregators. However, as demonstrated via numerical experiments, under stable dynamic pricing and DR strategies, the average difference between the cost and the revenue reduces to at or near zero. The SO (a non-profit agent) should neither accumulate excess revenue nor incur deficit.

3. Numerical implementation

In this section, we demonstrate our methodology by implementing it on a sample network with congestion as described below. We conducted our numerical study in two parts. First, for given load compositions and generator bids in DA and RT markets, we determine stable dynamic pricing and DR strategies. Thereafter, we examine the convergence of price and the corresponding load balancing profile over 24 hours, and also analyze the impact of the percentage of deferable loads in the network on the average dynamic price.

3.1. Sample network: A modified PJM 5-bus system

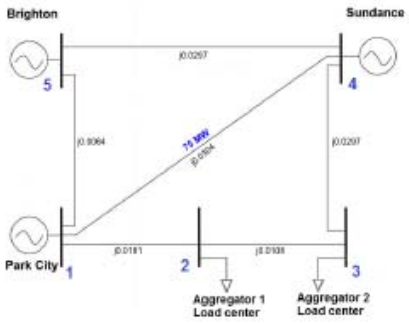

Fig. 3. Modified 5-bus PJM network

We use a minor variant of the PJM 5 bus system with 3 generators, 2 load nodes, and 6 transmission lines as shown in Fig. 3. The parameters a and b of the generators' DA supply offers (see Section 2.2) are (0.009, 47), (0.007, 35), and (0.005, 10.25), representing high, medium, and low cost generators at nodes 1, 5, and 4, respectively; corresponding parameter values for the real-time bids are (0.04, 80), (0.035, 70) and (0.03, 60). The maximum generating capacities are 2000, 2000 and 600 MW for generators at nodes 1, 4, and 5. The reactance of the transmission lines are as marked (see Fig. 3). We consider that the capacity of line connecting buses 1 and 4 is limited to 75 MW, and the remaining lines are unconstrained. The two load nodes are located at buses 2 and 3. In each of these load nodes, DR decisions are made by the respective aggregators.

We make the following assumptions about the load composition of the network.

The loads consist of entities and each entity comprises a number of households and businesses. There are 60 and 40 entities in node 2 (managed by aggregator 1) and node 3 (managed by aggregator 2), respectively. Each entity has non-deferrable (fixed) and deferrable (shiftable and shift-adjustable) loads. It is assumed that distribution of the hourly consumption levels of the fixed loads for all entities at a node can be approximated by a normal distribution. Fig. 4 depicts the mean and the one standard deviation confidence bounds of the hourly fixed loads at node 2. Similar load pattern is considered for fixed loads at node 3. As seen from the figure, the time of operation of the fixed loads are chosen to mimic the two-peak load pattern commonly observed in power networks.

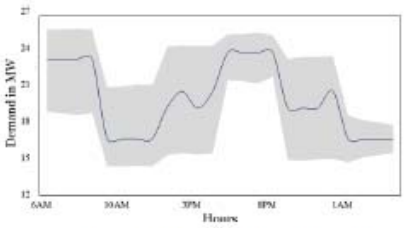

Fig. 4. Fixed load pattern for aggregator 1 at load node 2

There are three shiftable loads for each entity under aggregator 1, whose consumption levels are 2 MW/h, 3.7 MW/h and 5 MW/h. Each of these shiftable loads runs for a total 3 hours a day, where the hours could be non-contiguous. Shiftable load levels managed by aggregator 2 are 1.5 MW/h, 2 MW/h, 3.7 MW/h and 5 MW/h, each with a 3-hour non-contiguous operating time. All entities under both aggregators are considered to have two shift-adjustable loads. When operating, the maximum (minimum) energy consumption levels per hour for these loads are 1.5 (1.05) MW and 5 (3.5) MW. These loads can be run during any non-contiguous hours of the day as long as the total consumption per day reaches 6 MWh and 20 MWh.

3.2. Discussion of numerical results

Since DA demand prediction is critical to the success of the dynamic pricing and DR methodology, we first examine the performance of the Bayesian prediction model. The predicted demand is used by the SO to determine the DA prices, which in turn

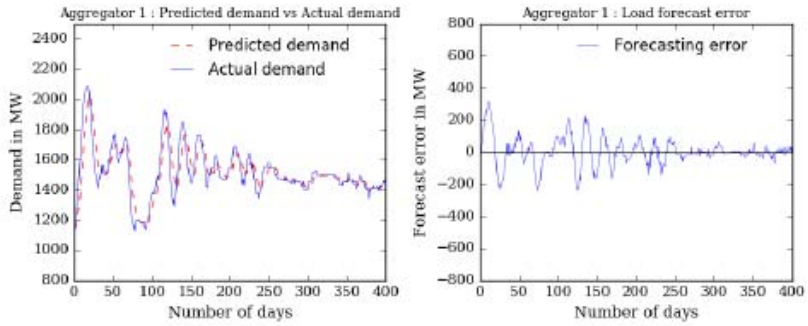

Fig. 5. Performance of Bayesian model for aggregator 1 at hour 10 AM

help to yield the hourly dynamic prices. We then discuss the efficacy of the estimation process for π_t^{max}, which is a key parameter for the robust DR model. In the remaining part of this section, we discuss the evolution of the dynamic pricing and DR strategies over the offline learning period of the methodology, followed by a brief sensitivity study.

Fig. 5 demonstrates the performance of the Bayesian model in predicting the DA demand for aggregator 1. The model predicts hourly demands for all 24 hours, of which the data for hour 10 AM is shown in the figure. It can be observed that during the initial days of simulated learning, due to aggregator's DR actions, the predicted DA demand vary significantly from the actual demand. As the variations in actual demand due to DR actions subside, the prediction error reduces to a very small value. A very similar behavior is also observed for the demand prediction by aggregator 2.

Before discussing the evolution of prices and consumption pattern in the network, we describe a key parameter of the robust DR model, π_t^{max}. It is the $100 \times (1 - \alpha)\%$ upper bound of the distribution of the historical values of dynamic prices π_t, and is the maximum possible price at a future hour t. This parameter plays a critical role in setting the level of risk considered by the robust DR model. Hence, a proper choice of π_t^{max} is essential to control how conservative we desire our DR actions to be. Unlike robust models commonly found in the literature, we continuously update π_t^{max}

at every iteration of the offline learning using newly available dynamic price data. At the beginning of the learning period, there is no available history of dynamic prices for the network and hence no initial estimate of π_t^{max}.

Therefore, for learning on day 1, we generate a history by drawing samples from a normal distribution with the DA price of day 1 as the mean and an assumed standard deviation ($4.0/MWh). The $100 \times (1 - \alpha)\%$ bound of this generated history is considered to be the π_t^{max}. On day 2 onwards, the dynamic price of the preceding day is added to the history and π_t^{max} is recalculated. Fig. 6 depicts the evolution of π_t^{max} for an arbitrarily chosen hour (11 AM) over the days of simulated learning. As expected, with learning, π_t^{max} approaches the dynamic price π_t.The choice of this initial value of standard deviation is not critical since it is updated as more data is available with the progress of the learning process.

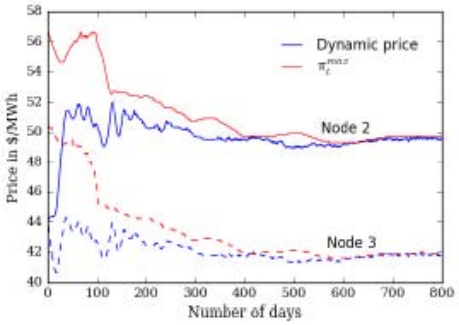

Fig. 6. Trend of π_t^{max} at hour 11 AM

3.2.1. Day-ahead, dynamic, and settled prices for the sample network

The simulated learning using our methodology is continued for a sufficiently large number of days until stable strategies arise with daily average dynamic prices sufficiently close to the daily average settled prices (DA and RT integrated LMPs). The parameter values used in our implementation are: $\alpha = .01$, $\gamma = 0.05$, and $\Gamma = 100\%$.

Fig. 7 depicts the evolution of the daily averages of day-ahead, dynamic, and settled prices at nodes 2 and 3 for over 600 days of simulation. The simulation was run for up to 1200 days, however, changes in prices are negligible after 600 days. As the two load nodes have different load characteristics and the network is subjected to congestion,

the price trajectories, as expected, are distinctly different. It can be seen from the figure that the performance of our methodology is not dependent on the choice of the dynamic prices for day 1. We chose, somewhat arbitrarily, identical starting dynamic prices ($44/MWh) for both nodes.

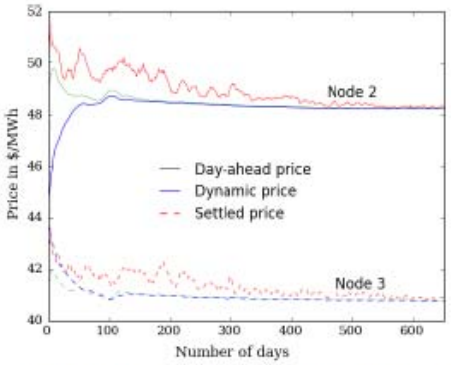

Fig. 7. Evolution of daily average values of day-ahead, dynamic, and settled prices

As observed, during the initial days of learning with limited available data, the prices vary significantly. This variation is caused by wide alteration in DR actions. We observed from our data, gathered during learning, that initial variations in DR produced higher demand peaks than usually observed in networks without dynamic pricing and DR. This confirms the fear that has been expressed in the literature [14]. However, as the offline learning of the dynamic prices continues over a sufficiently large number of days, the SO and the aggregators are able to learn stable and consistent dynamic pricing and corresponding DR strategies, respectively. This is manifested in the convergence of the day-ahead, dynamic, and settled prices. For example, after learning, the standard error (SE) between the settled and the dynamic prices reaches as low as 0.09%. Our methodology demonstrates that a real-world power network that implements dynamic pricing and aggregator guided demand response will not have to suffer through the long periods of price and demand uncertainties, and it can begin its operation with model-guided stable strategies. Table 1 shows the actual values of the stabilized hourly prices for both nodes.

Table 1 Hourly stabilized price for nodes 2 and 3

	Node 2 (Aggregator 1)					Node 3 (Aggregator 2)				
Hours	DAP $/MWh	DP $/MWh	SP $/MWh	SP-DAP $/MWh	SE(SP-DAP) $/MWh	DAP $/MWh	DP $/MWh	SP $/MWh	SP-DAP $/MWh	SE(SP-DAP) $/MWh
1	50.88	50.85	50.83	0.05560	0.12058	42.97	43.07	42.90	0.07821	0.30115
2	50.77	50.80	50.90	-0.13115	0.25232	42.90	42.91	42.93	-0.03059	0.56884
3	50.33	50.37	50.47	-0.13407	0.37648	42.50	42.57	42.72	-0.22751	0.75941
4	49.76	49.82	50.11	-0.35533	0.37592	41.97	42.01	42.05	-0.07857	0.69201
5	49.52	49.45	49.67	-0.15366	0.34717	41.78	41.96	42.10	-0.31128	0.49502
6	49.37	49.43	49.53	-0.15506	0.28856	41.66	41.62	41.63	0.03509	0.36658
7	49.29	49.21	49.30	-0.00453	0.15167	41.60	41.57	41.47	0.13486	0.28704
8	49.04	49.02	49.05	-0.01082	0.03019	41.38	41.40	41.52	-0.13367	0.06298
9	48.66	48.66	48.63	0.02757	0.07403	41.05	41.05	40.99	0.05815	0.05348
10	48.41	48.39	48.47	-0.06391	0.07190	40.84	40.85	40.88	-0.04590	0.06844
11	47.75	47.78	47.79	-0.03892	0.02081	40.29	40.30	40.35	-0.06450	0.04862
12	47.09	47.10	47.09	-0.00015	0.01648	39.71	39.72	39.71	-0.00124	0.00496
13	48.36	48.36	48.35	0.00215	0.00998	40.74	40.74	40.74	0.00064	0.00237
14	49.25	49.25	49.25	0.00018	0.00884	41.55	41.54	41.55	0.00023	0.00326
15	49.07	49.08	49.07	0.00411	0.00966	41.39	41.38	41.39	0.00003	0.00260
16	49.17	49.18	49.18	-0.00250	0.00929	41.47	41.47	41.47	0.00014	0.00111
17	46.21	46.21	46.22	-0.01254	0.02249	38.96	38.96	38.94	0.01301	0.01783
18	46.18	46.17	46.17	0.00922	0.02895	38.93	38.92	38.93	0.00056	0.00252
19	46.18	46.18	46.19	-0.00821	0.02777	38.93	38.94	38.93	0.00046	0.00374
20	46.12	46.12	46.12	0.00187	0.01223	38.88	38.89	38.88	0.00022	0.00351
21	45.99	45.99	45.98	0.00098	0.01007	38.76	38.77	38.76	0.00212	0.01671
22	45.94	45.94	45.94	0.00144	0.00707	38.72	38.72	38.72	0.00171	0.00194
23	45.92	45.92	45.92	-0.00045	0.00626	38.71	38.71	38.71	0.00210	0.00339
24	45.91	45.91	45.91	-0.00059	0.00224	38.70	38.70	38.70	0.00074	0.00044

Note: DAP - DA price; DP - Dynamic price; SP - Settled price

3.2.2. Load distribution at the nodes resulting from DR

Influence of dynamic pricing and corresponding DR actions on the daily demand patterns and load factors at the two load nodes are depicted in Fig. 8. The plots on the left exhibit the initial ad-hoc demand patterns that are simulated to mimic the two peak demand patterns observed in real networks. Bars represent the fixed load. The red dotted line represents the ad-hoc total demand pattern combining the fixed and deferrable loads. The stable demand pattern achieved using DR is shown by the blue dotted line. Clearly, the deferrable portion of the initial demand pattern is redistributed from high to low demand periods by the DR actions, yielding a lower PAR (peak to average ratio) value. The plots on the right demonstrate the evolution of the load factor (ratio of average load to maximum load of a day) over the learning period. It is considered in the sample network problem that between 10% to 15% of its daily loads

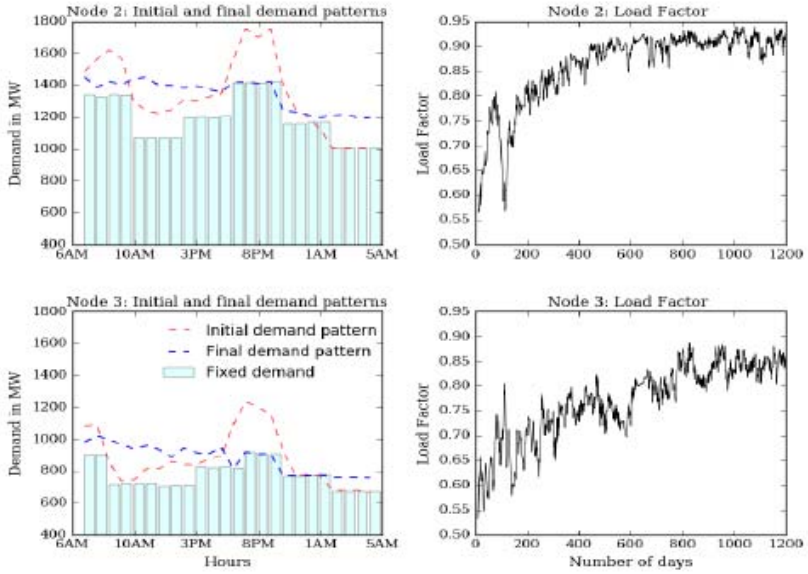

Fig. 8. Load pattern and corresponding load factors

are deferrable. Despite the small proportion of deferrable loads, due to the fluctuations in the DR actions in the initial learning stages, the load factors are at very low values near 0.55. As the learning progresses and the DR actions stabilize, the load factors improve to near 0.9.

3.2.3. Sensitivity of the proportion of deferrable loads

We studied the impact of the percentage of deferrable loads in the network on the average daily dynamic price and the load factor. Table 2 shows that even for a small level of deferrable load (5 - 7 %), a stable dynamic pricing and DR strategy improves the load factor by about 10% compared to the scenario with no DR. Also, the load factor and price improves with the increase in the percentage of deferrable loads. This shows that both power networks as well as the consumers could benefit by being more flexible, i.e., designating more of their loads as deferrable.

Table 2 Effect of the level of deferrable load on load factor and average dynamic price

% of Deferrable load participation	Node 2 (Aggregator 1) Load factor	Avg.Dynamic price $/MWh	Node 3 (Aggregator 2) Load factor	Avg.Dynamic price $/MWh
0 (no DR)	0.7678	-	0.7109	-
5-7	0.8588	48.47	0.806	40.92
10-12	0.9192	48.24	0.8607	40.75
14-16	0.946	48.16	0.87331	40.75

4. Conclusions

This paper presents a new data driven offline methodology that simulates power networks that operate with dynamic pricing and demand response. An application on a congested network shows that it is possible to obtain stable strategies for dynamic pricing and DR that can improve load balance in the network and reduce cost to the consumers. This helps to dispel the common apprehension that dynamic pricing and DR could increase electric power market volatility and reduce network reliability. It is also evident from our results that it is viable for SO to offer binding dynamic prices ahead of consumption. The methodology learns offline without disrupting actual network operations. For any change in the network configuration and other parameters (e.g., DA and RT price bids), the simulation can be rerun and new strategies can be learned. The sensitivity analysis shows that there is a financial motivation for the consumers to designate more of their loads as deferrable, as DR yields lower average prices of electricity.

Examination of the Bayesian demand prediction model (Fig. 5) shows that it is able to incorporate varying demand from DR actions in the learning process and improve its prediction to reduce forecasting error. In addition to effective demand forecasting, the other aspect of our methodology that helps the dynamic prices to reach stable values is the evolution of the π_t^{max} term in the robust DR model (see Fig. 6). A game theoretic optimization approach to obtain stable dynamic pricing and DR actions for a network

can be found in [34]. The findings of our data-driven methodology is similar to that in [34], which also obtains stable policies while maintaining the revenue neutral status of SO, balancing network load, and reducing cost to consumers.

References

[1] S. Borenstein, Time-varying retail electricity prices: Theory and practice, Electricity deregulation: choices and challenges:University of Chicago Press (2005) 317–357.

[2] S. Borenstein, M. Jaske, A. Rosenfeld, Dynamic pricing, advanced metering, and demand response in electricity markets, Center for the Study of Energy Markets, UC Berkeley, (2002).

[3] G. Dutta, K. Mitra, A literature review on dynamic pricing of electricity, Journal of the Operational Research Society 68 (10) (2017) 1131–1145.

[4] A. R. Khan, A. Mahmood, A. Safdar, Z. A. Khan, N. A. Khan, Load forecasting, dynamic pricing and dsm in smart grid: A review, Renewable and Sustainable Energy Reviews 54 (2016) 1311–1322.

[5] A. Faruqui, J. Palmer, The discovery of price responsiveness–a survey of experiments involving dynamic pricing of electricity. Brattle group; 2012.

[6] S. Borenstein, Effective and equitable adoption of opt-in residential dynamic electricity pricing, Review of Industrial Organization 42 (2) (2013) 127–160.

[7] F. Ahmad, The ethics of dynamic pricing, Electrical Journal 23 (2010) 13–27.

[8] D. Zhou, M. Roozbehani, M. A. Dahleh, C. J. Tomlin, Stability analysis of wholesale electricity markets under dynamic consumption models and real-time pricing, arXiv preprint arXiv:1609.06193.

[9] J. D. Quillinan, Pricing for retail electricity, Journal of Revenue and Pricing Management 10 (6) (2011) 545–555.

[10] A. Faruqui, S. Sergici, L. Akaba, The impact of dynamic pricing on residential and small commercial and industrial usage: New experimental evidence from connecticut, The Energy Journal (2014) 137–160.

[11] M. Zugno, J. M. Morales, P. Pinson, H. Madsen, A bilevel model for electricity retailers' participation in a demand response market environment, Energy Economics 36 (2013) 182–197.

[12] M. Alizadeh, X. Li, Z. Wang, A. Scaglione, R. Melton, Demand-side management in the smart grid: Information processing for the power switch, IEEE Signal Processing Magazine 29 (5) (2012) 55–67.

[13] M. Roozbehani, M. A. Dahleh, S. K. Mitter, Volatility of power grids under real-time pricing, IEEE Transactions on Power Systems 27 (4) (2012) 1926–1940.

[14] S. D. Ramchurn, P. Vytelingum, A. Rogers, N. Jennings, Agent-based control for decentralised demand side management in the smart grid, in: The 10th International Conference on Autonomous Agents and Multiagent Systems-Volume 1, International Foundation for Autonomous Agents and Multiagent Systems, 2011, pp. 5–12.

[15] M. Muratori, B.-A. Schuelke-Leech, G. Rizzoni, Role of residential demand response in modern electricity markets, Renewable and Sustainable Energy Reviews 33 (2014) 546–553.

[16] A. Faruqui, A. Hajos, R. Hledik, S. Newell, Fostering economic demand response in the Midwest ISO, Energy 35 (4) (2010) 1544–1552.

[17] L. Gkatzikis, I. Koutsopoulos, T. Salonidis, The role of aggregators in smart grid demand response markets, IEEE Journal on Selected Areas in Communications 31 (7) (2013) 1247–1257.

[18] M. Beaudin, H. Zareipour, Home energy management systems: A review of modelling and complexity, Renewable and Sustainable Energy Reviews 45 (2015) 318–335.

[19] R. Missaoui, H. Joumaa, S. Ploix, S. Bacha, Managing energy smart homes according to energy prices: Analysis of a building energy management system, Energy and Buildings 71 (2014) 155–167.

[20] M. Goulden, B. Bedwell, S. Rennick-Egglestone, T. Rodden, A. Spence, Smart grids, smart users? the role of the user in demand side management, Energy research & social science 2 (2014) 21–29.

[21] P. Samadi, H. Mohsenian-Rad, V. W. Wong, R. Schober, Real-time pricing for demand response based on stochastic approximation, IEEE Transactions on Smart Grid 5 (2) (2014) 789–798.

[22] C. Zhang, Q. Wang, J. Wang, P. Pinson, J. M. Morales, J. Østergaard, Real-time procurement strategies of a proactive distribution company with aggregator-based demand response, IEEE Transactions on Smart Grid 9 (2) (2018) 766–776.

[23] C. Gorria, J. Jimeno, I. Laresgoiti, M. Lezaun, N. Ruiz, Forecasting flexibility in electricity demand with price/consumption volume signals, Electric Power Systems Research 95 (2013) 200–205.

[24] M. Muratori, G. Rizzoni, Residential demand response: Dynamic energy management and time-varying electricity pricing, IEEE Transactions on Power systems 31 (2) (2016) 1108–1117.

[25] D. Setlhaolo, X. Xia, J. Zhang, Optimal scheduling of household appliances for demand response, Electric Power Systems Research 116 (2014) 24–28.

[26] A. Fakhrazari, H. Vakilzadian, F. F. Choobineh, Optimal energy scheduling for a smart entity, IEEE Transactions on Smart Grid 5 (6) (2014) 2919–2928.

[27] R. Dhulst, W. Labeeuw, B. Beusen, S. Claessens, G. Deconinck, K. Vanthournout, Demand response flexibility and flexibility potential of residential smart appliances: Experiences from large pilot test in belgium, Applied Energy 155 (2015) 79–90.

[28] K. Vanthournout, B. Dupont, W. Foubert, C. Stuckens, S. Claessens, An automated residential demand response pilot experiment, based on day-ahead dynamic pricing, Applied Energy 155 (2015) 195–203.

[29] B. Stott, O. Alsac, Fast decoupled load flow, IEEE transactions on power apparatus and systems (3) (1974) 859–869.

[30] X. Cheng, T. J. Overbye, An energy reference bus independent lmp decomposition algorithm, IEEE Transactions on Power Systems 21 (3) (2006) 1041–1049.

[31] A. Magnani, S. P. Boyd, Convex piecewise-linear fitting, Optimization and Engineering 10 (1) (2009) 1–17.

[32] M. Roozbehani, M. Dahleh, S. Mitter, Dynamic pricing and stabilization of supply and demand in modern electric power grids, in: Smart Grid Communications (SmartGridComm), 2010 First IEEE International Conference on, IEEE, 2010, pp. 543–548.

[33] D. Bertsimas, M. Sim, Robust discrete optimization and network flows, Mathematical programming 98 (1) (2003) 49–71.

[34] V. Subramanian, T. K. Das, A two-layer model for dynamic pricing of electricity and optimal charging of electric vehicles under price spikes, (2018), `http://vigneshs.myweb.usf.edu/publications/index.html/`, accessed: September, 11, 2018.

Appendix D: Published Material in Energy Journal

Energy 167 (2019) 1266–1277

Contents lists available at ScienceDirect

Energy

journal homepage: www.elsevier.com/locate/energy

A two-layer model for dynamic pricing of electricity and optimal charging of electric vehicles under price spikes

Vignesh Subramanian*, Tapas K. Das

Department of Industrial and Management Systems Engineering, University of South Florida, Tampa, FL, 33620, USA

ARTICLE INFO

Article history:
Received 23 August 2018
Received in revised form
10 October 2018
Accepted 27 October 2018
Available online 2 November 2018

Keywords:
Dynamic pricing
Electric vehicles
Demand response
Mathematical program with equilibrium constraints
Robust optimization

ABSTRACT

Pilot projects in power networks conducted across continents have established the benefits of dynamic pricing by inducing increased demand response. However, a key hurdle in the growth of demand response is the lack of widespread availability of advanced metering infrastructure, which has stymied the adoption of dynamic pricing. We believe that this hurdle will be partially addressed by the growth of electric vehicles (EVs), as smart and connected EV parking lots will be a provider of demand response. We develop a two-layer optimization model that simultaneously determines dynamic pricing policy for the system operator and demand response strategies for the EV parking lots. The model minimizes the cost to consumers, while ensuring the system operator's revenue neutral status and addressing real-time price uncertainties. A variant of the 5-bus PJM network is used to demonstrate model implementation. Numerical results show that for a low to moderate price spike scenario, dynamic pricing with demand response from EVs alone can lower the daily average consumer cost of 1.42% compared to the cost of flat pricing. A cost reduction of 6.5% is achieved when price spikes are relatively high. Computational challenges of implementing our model for real networks are discussed in the concluding remarks.

1. Introduction

It was recommended early in the new millennium that power networks will benefit significantly from dynamic pricing and demand response [1]. Some of the recent review papers that futher emphasize this are [2–4]. Till date, dynamic pricing policies have remained limited to variants of time of use (TOU), critical peak pricing (CPP), and ex-post real time pricing (RTP). The lack of availability of a pure form of dynamic pricing, where binding prices are offered to consumers just ahead of power usage, has limited the incentives for demand response to grow. As a result, historically, hourly demand for electricity has remained highly uneven and has continued to cause significant price spikes. It is estimated that networks maintain 10–15% of the average demand as reserve capacity to deal with uneven load distribution. Also, 10% of the cost of electricity is spent in 1% of the operating times due to price spikes [5,6]. For example, in the month of May 2018, the price of electricity in the ERCOT market in the U.S. spiked from the average level of $25-$60/MWh to $750-$1600/MWh. During the same period the price in the NYISO market in the U.S. experienced price fluctuations in the range of -$600/MWh to $1000/MWh [7]. The woes of power networks may be exacerbated in coming years with the explosion of EVs and resulting increase in energy demand as well as change in daily load patterns. It is estimated that the number of EVs will grow to 7.3 million by 2023 in the U.S. [8]. Considering an average battery capacity of 70 kWh, charging of these batteries even once a day may consume up to an additional 500,000 MWh. Unless managed well, this consumption growth could significantly alter the current daily load profile and further increase price spikes. We recognize, however, that the growth of EVs will also bring an unique opportunity for increased demand response. Large number of EVs will be parked in smart, connected, and aggregator managed parking lots. While parked, these EVs will be charged optimally and thus will likely shift EV demand to off-peak periods and reduce stress on the network.

In this paper we present a two-layer optimization model to develop policies for implementing pure dynamic pricing of electricity and demand response using EVs. The top-layer of our model addresses the day-ahead (DA) market operations using a two-stage stochastic model that considers different demand patterns and uncertain real-time (RT) prices. The RT market operations, using DA solutions as an input, are considered in the bottom-layer and are

* Corresponding author.
E-mail address: vigneshs@mail.usf.edu (V. Subramanian).

https://doi.org/10.1016/j.energy.2018.10.171
0360-5442/

formulated as a bilevel model which is solved for each hour of the day, just before dispatch. The upper-level of the bilevel model solves for dynamic prices and the lower-level determines the demand response action (optimal charging).

The important features of our two-layer model are the following: 1) the top-layer model considers power network configurations including congestion, 2) the bilevel model uses a robust optimization framework to accommodate RT price uncertainties, 3) the upper-level of the bilevel model uses a specific constraint to manage revenue neutrality of the system operator (SO), 4) a mixture of two probability distributions is used to generate price spikes, their magnitude and time of occurrence and 5) a granular parking lot model with a large volume of EVs comprising different makes, models, battery capacities, and charging needs. As regards solution of the model, we first reformulate the bilevel model into a single level mathematical program with equilibrium constraints (MPEC) model. We then linearize the MPEC model using the strong duality principle. The resulting optimization model is a single level mixed integer linear programming (MILP), which is solved using a conventional approach. In the rest of this section, a short review of literature on dynamic pricing and demand response is presented.

A pure form of dynamic pricing, where binding prices are declared just ahead of consumption in small intervals (say, an hour or less), is often referred to in the literature as real time pricing, RTP. However, the nomenclature of dynamic pricing and RTP is used widely in the literature to include many other forms of time varying pricing strategies. Such strategies include: block rate tariffs, seasonal tariffs, TOU, superpeak TOU, CPP, variable peak pricing (VPP), and RTP; see Ref. [2] for definitions of these pricing schemes. Henceforth, in this paper, we will only consider the pure form of dynamic pricing that offers binding prices ahead of consumption. Implementation of this dynamic pricing requires availability of advanced metering infrastructure (AMI). Literature shows that availability of smart technology increases price elasticity and grid efficiency [9–11]. Beneficial impacts of dynamic pricing have been explored through many pilot projects in recent years. The survey presented in Ref. [12] examined seventy-four dynamic pricing experiments across three continents during the last decade. The results show that increase in price peaks offers better benefits of load balancing from dynamic pricing. It is shown in Ref. [13] that dynamic pricing can achieve a peak demand reduction of 10–14%, customer cost reduction of 2–5%, and a social welfare increase by $141-$403 million in a year. A study conducted in California [14] found that most consumers will benefit from dynamic pricing, and also that low income consumers will not be impacted negatively, a concern that was expressed earlier. Even with well documented benefits of dynamic pricing, its implementation in power network still remains a challenge. This is due to the lack of adoption of AMI, and, to our knowledge, need for models that can yield appropriate dynamic pricing strategies for networks affected by price volatility.

Though broad availability of AMI for consumers to engage in demand response remains a capital investment challenge, a significant number of papers have been presented to the literature that address demand response by residential thermostatic loads and distributed generation. In Ref. [15], a two-stage stochastic optimization model is developed for the aggregators to optimally control flexible thermostatic loads (e.g., water and space heaters) and buy back from prosumers' storage to trade in spot markets to minimize overall cost. The same authors in Ref. [16] considered a multi-stage stochastic modeling approach for the aggregators to minimize prosumers' cost by bidding sequentially in the option market, DA market, and near RT market. In the model presented in Ref. [17], the aggregators first determine the DA quantity considering EV, thermostatic loads, shiftable load, and renewable generation. Thereafter, a model predictive control approach is used to adjust the flexible loads to minimize the net cost of buying and selling energy in the RT market. It is claimed that this strategy reduces the net cost of aggregators by 14% compared with operation with no DR. A bi-objective optimization model in Ref. [18] develops a tradeoff between user comfort and cost of energy consumption in smart buildings. It is shown in Ref. [19] that a 17% energy cost saving can be attained through DR in residential microgrids equipped with photovoltaic systems, flexible loads, and electric vehicles. The savings can be further increased by 6% if battery storage is available. A recent paper in Ref. [20] obtains simultaneous strategies for dynamic pricing by SO and demand response by load aggregators using a data driven iterative learning approach.

We believe that the impending growth of EVs will bring new opportunities for power networks as the aggregator managed EV parking lots will supplement the existing modes of demand response. The technical and economical feasibility of incorporating EV aggregator as a resource to the network is addressed in Ref. [21]. A conceptual regulatory framework and a business model to integrate EVs in the network and in turn support the power system operation is proposed in Ref. [22]. In Ref. [23], the authors propose an aggregated EV charging schedule in coordination with the SO. It is claimed that such charging schedules will enhance the grid efficiency and security, and thus allow significant EV penetration without a need for grid capacity expansion. Optimal and risk averse bidding strategies for EV aggregators under the constraints of market uncertainty, EV owners' behavior, and aggregators' profit volatility are presented in Refs. [24–26]. In Ref. [27], a stochastic programming methodology is developed with an objective of maximizing aggregator profit by charging the EVs on low price periods under time-varying market prices. They show that if the uncertainty in the number of vehicles in the parking lots is ignored, the aggregator profit is overestimated by 23.8%. A stochastic model from the SO's perspective in Ref. [28] incorporates demand response offered by the EVs. The model shows that SO can minimize the operation cost by optimally scheduling conventional generators, and the aggregators can minimize the electricity payment through DR participation. The objective of minimizing the cost of EV parking lot operation was approached via a cooperative game model in Ref. [29] and a non-cooperative game model in Ref. [30]. The cooperative game model reduced the cost through negotiation with the utility and the non-cooperative model used a price-driven EV charging model. A decentralized pricing scheme is proposed in Ref. [31], where SO sends the price and quantity information to the load aggregator, and both parties iteratively reoptimize the system dispatch and EV charging. A bilevel model is proposed in Ref. [32] that captures the interactions between the SO and parking lots. The model determines the scheduled energy for the parking lots based on the price offered by SO. Results show that the SO could achieve a considerable reduction of 8–9% of its total daily operation cost through parking lots' participation in the reserve market. In another bilevel model [33], the interaction between an EV aggregator and a parking lot owner is examined.

We make two key observations from the literature reviewed above. First, pure dynamic pricing has long been recommended as an enabler for demand response. Many pilot projects in the U.S. and Europe have demonstrated the expected benefits of pure form of dynamic pricing. However, there is a gap in the literature for model-based support on how to develop strategies for dynamic pricing for different network structure and composition. The second observation is that though models for various aspects of EVs have been presented to the literature, to our knowledge, a model for EV integration under dynamic pricing has not yet been made openly available. Our paper addresses both of the observations.

The remaining paper is organized as follows. Section 2 describes the modeling approach. The two-layer model is presented in

Section 3. In Section 4, the model is implemented on a sample 5-bus PJM network with actual load data from PJM zones. Performance comparison of dynamic pricing and demand response strategies with other existing and adhoc policies is also given in Section 4. Concluding remarks are contained in Section 5.

2. Modeling approach

Our two-layer modeling approach is depicted in Fig. 1. Before discussing the model elements, we state some of the modeling considerations and limitations. The financial settlement occurs in two stages: in the DA and the RT markets. The SO determines the dynamic prices by considering the possible outcomes of both markets. Strategic aggregators manage the loads in the network that include fixed residential and business loads, and schedulable EV loads in large parking lots. These parking lots host a variety of vehicles with different battery types at different times of the day and for different periods of stay. EVs arrive and depart with different charge levels. Depending on the hourly price variation, the aggregators develop their demand response strategies by optimally deciding charging schedules for the EVs. We assume the time interval to be an hour. One limitation of our model is that the aggregators neither inject power back from the vehicles to the grid (V2G) nor engage in any other forms of temporal arbitrage for peer-to-peer trading. Under present electricity pricing policies and some of the prevailing battery technologies (e.g., lead-acid, NiMH), V2G operation is still considered not cost effective [34]. However, evolving battery technologies, like lithium ion, can withstand charge cycling and support V2G.

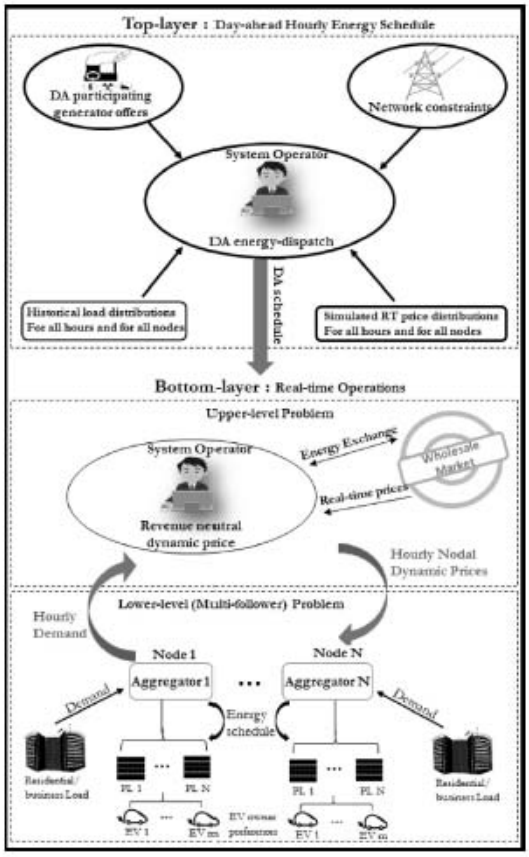

Fig. 1. Model components and their interactions.

The top-layer determines the DA quantities and prices for all hours of the day using DA generators' supply bids, historical demand patterns, and the corresponding RT prices. The model uses a network constrained least-cost dispatch principle for market clearing and is formulated as a two-stage stochastic program. The first stage determines the energy procured in the DA market, and the second stage decides the RT quantities. The RT prices are subjected to price spikes and are considered exogenous. The solution of the two-stage program yields scheduled DA hourly quantities and locational marginal prices (LMPs). These DA quantity-price pairs are sent to the bottom-layer model as input.

The bottom-layer is a bilevel model and is solved at the beginning of every hour. In the upper-level, the SO determines the dynamic prices for the hour using the lower-level problem as constraint. It minimizes the total cost of satisfying demands for the current and the future hours of the day, while meeting the key constraint of SO being revenue neutral. The RT prices are assumed to be known for the current hour, while the future hour RT prices are considered unknown and are modeled as uncertainty sets using a robust approach. The lower-level represents multiple aggregators (one for each load node) and obtains the optimal demand response actions. This is achieved by considering dynamic prices for the current hour and the DA prices as the estimates for the future hours. In what follows, we present a general framework for the two-layer model before presenting the complete model in the next section.

For the top-layer model, let c^N denote the supply offer of the generators and λ_ω^N denote the real-time prices for demand scenario ω. The decision variables for the energy procured in the DA and RT markets are denoted by E^{DA} and E_ω^{RT}, respectively. The probability distribution of each demand scenario is denoted by π_ω. The first constraint represents the first stage DA market operation and considers power balance, generator output, and transmission line limits. The dual variable (DA price) corresponding to the first stage constraint is denoted by λ^{DA}. The second constraint ensures the power balance in the RT market for all realizations ω of demand. The solution of the top-layer denoted by $\widehat{E}^{DA}$ and $\widehat{\lambda}^{DA}$ are sent to the bottom-layer. For simplicity, the index for time intervals of the day is omitted from the general formulation.

$$\text{Top}-\text{layer}\begin{cases}\min\limits_{E^{DA},E_\omega^{RT}} c^N E^{DA}+\sum\limits_{\omega\in\Omega}\pi_\omega\lambda_\omega^N E_\omega^{RT}, & \\ \text{s.t.} & \\ A^T E^{DA}\geq b, & \left(\lambda^{DA}\right)\\ p_\omega E^{DA}+q_\omega E_\omega^{RT}\geq\xi_\omega, & \forall\,\omega\in\Omega\\ E^{DA}\geq 0,\ E_\omega^{RT}\geq 0. & \forall\,\omega\in\Omega\end{cases}\tag{1}$$

$$\text{Bottom}-\text{layer}\begin{cases}\min\limits_{x\in X} F\left(x,y_1,\cdots,y_k\middle|\widehat{E}^{DA},\widehat{\lambda}^{DA}\right), & \\ \text{s.t.} & \\ G\left(x,y_1,\cdots,y_k\middle|\widehat{E}^{DA},\widehat{\lambda}^{DA}\right)\leq 0, & \\ y_i=\operatorname{argmin} f_i\left(x_i,y_i\middle|\widehat{\lambda}^{DA}\right), & \forall i=1,\cdots,k\\ g_i(x_i,y_i)\leq 0. & \forall i=1,\cdots,k\end{cases}\tag{2}$$

In the bottom-layer model, $x\in\mathbb{R}^k$ and $y_i\in\mathbb{R}$ are the decision

variables representing hourly dynamic prices (upper-level) and each aggregator's consumption (lower-level), respectively, where k denotes the number of aggregators (followers) in the network. The SO's objective function in the upper level, $F:\mathbb{R}^{2k}\rightarrow\mathbb{R}$, is to optimally procure energy in DA and RT markets. The objective function of the i^{th} aggregator at the lower level, $f_i:\mathbb{R}^2\rightarrow\mathbb{R}$, aims to minimize the total cost of energy consumption for the given dynamic price x_i. The upper and lower level constraints are denoted as $G(\cdot)$ and $g_i(\cdot)$, respectively.

The uniqueness of the above bilevel model is that it has multiple followers at the lower-level, and each follower's decision variable and the associated strategy space are independent of those of the other followers. The bilevel model can be reformulated as a single level MPEC as in Refs. [35,36] and are used in our solution approach. The lower-level model is linear and convex, and is reformulated as Karush-Kuhn-Tucker (KKT) optimality conditions (referred to as mathematical program with equilibrium constraint, MPEC). Big-M method and strong duality principle are used to linearize the model and thus obtain the equivalent single level MILP optimization model that can be solved using conventional approaches.

3. The model

In this section we present the details of the top and bottom-layer optimization models. As stated earlier, the top-layer is a two-stage stochastic model, and the bottom-layer is a bilevel robust optimization model.

3.1. Top-layer model

The top-layer concerns the DA market, where the SO decides the optimal DA scheduled quantities. The SO considers historical scenarios of demand patterns and corresponding RT prices at each node, together with the generator DA bids to determine the optimal DA schedule quantities. This is accomplished via a two-stage stochastic model where the first stage decides the DA quantities and the second stage obtains the RT quantities for all possible scenarios. The objective function minimizes the total expected cost of energy purchased in the DA and RT markets for all load nodes ($N_L \subset N$) and for all hours T. The term $C_g^{DA}(\cdot)$ denotes the cost function of participating generator $g \in N_G$ in the DA market. The decision variable for the generator output in the DA market is denoted by P_{gt}. The additional quantities purchased in the RT market in demand scenario ω (with probability π_ω) is denoted by $P_{gt}^{\omega,\Delta+}$. If the DA quantity exceeds demand in scenario ω, then the excess amount, denoted by $P_{gt}^{\omega,\Delta-}$, is assumed to be sold in the RT market. The RT price at node n and time t under demand scenario ω is denoted by $\lambda_{nt}^{RT,\omega}$.

Constraint (3) ensures the first stage network power balance. Let N_G^n denote the subset of the generators that are at node n, and B_n denote the set of nodes in the network that are directly connected to node n. For $m \in B_n$, let b_{nm} denote the susceptance of the line between the nodes n and m, and δ_{nt} denote the voltage angle (in radians) at node n and time t. The term E_{nt}^{DA} represents the scheduled DA quantity for the load node n and time t. Constraints (4) and (5) represent transmission line flow limits and generator output limits, respectively; $\overline{F}_{nm}$ represents the maximum line flow in MW, and $\underline{P}_g$ ($\overline{P}_g$) are lower (upper) limit of generator real power output in MW. Constraint (6) is used to designate node 1 as a reference bus (or slack bus) in the network. Constraint (7) ensures all other node buses are within the voltage angle limits.

$$\min \sum_{t=1}^{T}\left[\sum_{g\in N_G} C_g^{DA}(P_{gt}) + \sum_{\omega\in\Omega}\pi_\omega \sum_{n\in N}\left\{\lambda_{nt}^{RT,\omega}\sum_{g\in N_G^n}\left(P_{gt}^{\omega,\Delta+} - P_{gt}^{\omega,\Delta-}\right)\right\}\right]$$

s.t.

First stage constraints

$$\sum_{g\in N_G^n} P_{gt} + \sum_{m\in B_n} b_{nm}[\delta_{nt} - \delta_{mt}] - E_{nt}^{DA} = 0, \quad \forall n\in N, \forall t\in T \tag{3}$$

$$-\overline{F}_{nm} \le b_{nm}[\delta_{nt} - \delta_{mt}] \le \overline{F}_{nm}, \quad \forall m\in B_n : m<n, \forall n\in N, \forall t\in T \tag{4}$$

$$\underline{P}_g \le P_{gt} \le \overline{P}_g, \quad \forall g\in N_G, \forall t\in T \tag{5}$$

$$\delta_{1t} = 0, \quad \forall t\in T \tag{6}$$

$$-\pi \le \delta_{nt} \le \pi, \quad \forall n\in N, \forall t\in T \tag{7}$$

Second stage constraints

$$\sum_{g\in N_G^n}\left(P_{gt}^{\omega,\Delta+} - P_{gt}^{\omega,\Delta-}\right) + \sum_{m\in B_n} b_{nm}\left[\delta_{nt}^{\omega} - \delta_{mt}^{\omega} - \delta_{nt} + \delta_{mt}\right] - \left(E_{nt}^{RT,\omega,\Delta^+} - E_{nt}^{RT,\omega,\Delta^-}\right) = 0, \quad \forall n\in N, \forall\omega\in\Omega, \forall t\in T \tag{8}$$

$$-\overline{F}_{nm} \le b_{nm}\left[\delta_{nt}^{\omega} - \delta_{mt}^{\omega}\right] \le \overline{F}_{nm}, \quad \forall m\in B_n : m<n, \forall n\in N, \forall\omega\in\Omega, \forall t\in T \tag{9}$$

$$\underline{P}_g \le P_{gt} + P_{gt}^{\omega,\Delta+} - P_{gt}^{\omega,\Delta-} \le \overline{P}_g, \quad \forall g\in N_G, \forall\omega\in\Omega, \forall t\in T \tag{10}$$

$$E_{nt}^{DA} + E_{nt}^{RT,\omega,\Delta^+} - E_{nt}^{RT,\omega,\Delta^-} = D_{nt}^{\omega}, \quad \forall n\in N_L, \forall\omega\in\Omega, \forall t\in T \tag{11}$$

$$E_{nt}^{DA} \ge \min_{\omega\in\Omega} D_{nt}^{\omega}, \quad \forall n\in N_L, \forall t\in T \tag{12}$$

$$E_{nt}^{DA} \le \max_{\omega\in\Omega} D_{nt}^{\omega}, \quad \forall n\in N_L, \forall t\in T \tag{13}$$

$$\delta_{1t}^{\omega} = 0, \quad \forall\omega\in\Omega, \forall t\in T \tag{14}$$

$$-\pi \le \delta_{nt}^{\omega} \le \pi, \quad \forall n\in N, \forall\omega\in\Omega, \forall t\in T \tag{15}$$

$$P_{gt}, P_{gt}^{\omega,\Delta+}, P_{gt}^{\omega,\Delta-}, E_{nt}^{DA}, E_{nt}^{RT,\omega,\Delta^+}, E_{nt}^{RT,\omega,\Delta^-} \ge 0$$

The remaining constraints are for the second stage model. Power balance for all RT demand realizations is ensured by constraint (8), where $E_{nt}^{RT,\omega,\Delta^+}$ and $E_{nt}^{RT,\omega,\Delta^-}$ are positive and negative demand deviations from the DA scheduled quantities. Constraint (9) and (10) are line flow and generator limits for all demand realizations. Constraint (11) ensures that total energy scheduled in the DA and RT markets matches the realized demand D_{nt}^{ω}. To ensure stable load scheduling, we have added constraints (12) and (13) such that the energy scheduled in the DA market is within the bounds of the realized demand. Constraints (14) and (15) represent the power angles for reference node and all other nodes, respectively. The dual variables of first stage constraints (3)-(5) can be decomposed into

marginal cost of energy at reference bus, marginal cost of power network losses, and cost of congestion, respectively. Using these dual values, the DA LMPs (denotes as λ_{nt}^{DA}) for all nodes and for all time periods are calculated. These LMPs and their associated quantities (E_{nt}^{DA}) are used as inputs in the bottom-layer model. Before presenting the bottom-layer model, we discuss how the RT prices ($\lambda_{nt}^{RT,\omega}$) are modeled using the approach in Ref. [37].

For each scenario ω, we solve the DCOPF model to get the market clearing prices (MCPs) at all nodes. We then express the RT prices as $\lambda_{nt}^{RT,\omega} = MCP_{nt}^{\omega}|1+\varepsilon|$, where $\varepsilon = M_1\varepsilon_1 + M_2\varepsilon_2$, and ε_1 and ε_2 are random variables, values of which are drawn from normal and Cauchy distributions with parameters (μ_1, σ_1) and (μ_2, σ_2), respectively; (M_1, M_2) is a bivariate random variable that takes values of (0,1) with probability p_s and (1,0) with probability $(1-p_s)$, where p_s is the probability of occurrence of price spikes. The normal random variable ε_1 contributes to the usual variability in the RT prices during off-peak periods, whereas the Cauchy random variable ε_2, chosen with probability p_s, generates the price spikes. Note that, the term ε and their related terms are also depend on node n and time t. For notation simplicity, the indexes are dropped.

3.2. Bottom-layer model

The bottom-layer is formulated as a bilevel model that is solved at the beginning of every hour. At the upper level, the SO determine appropriate dynamic prices at each load node for each hour, and at the lower level, the aggregators determine optimal consumption levels.

3.2.1. Upper-level model

The SO's goal in the model presented below is two-fold: 1) to minimize the total cost of satisfying the demand in the current and all future hours of the day, and 2) to ensure that the dynamic prices for the current hour are selected such that there is no significant revenue loss or surplus. Recall that the aggregators pay binding dynamic prices for the current hour, which may be different from the DA or RT prices. A robust approach is used to assess future RT prices.

$$\min \sum_{n\in N_L}\Bigg[\lambda_{n\tau}^{DA}E_{n\tau}^{DA} + \lambda_{n\tau}^{RT}\left(E_{n\tau} - E_{n\tau}^{DA}\right) + \sum_{t>\tau}^{T}\Bigg(\lambda_{nt}^{DA}E_{nt}^{DA} + \frac{1}{2}\left(\overline{\lambda}_{nt}^{RT} + \underline{\lambda}_{nt}^{RT}\right)\left(E_{nt} - E_{nt}^{DA}\right)\Bigg) + \Gamma_n^{RT}Z_n^{RT} + \sum_{t>\tau}^{T}\eta_{nt}^{RT}\Bigg],$$

s.t.

$$\pi_{n\tau}E_{n\tau} - \lambda_{n\tau}^{DA}E_{n\tau}^{DA} - \lambda_{n\tau}^{RT}\left(E_{n\tau} - E_{n\tau}^{DA}\right) \geq 0, \qquad \forall n\in N_L \tag{16}$$

$$Z_n^{RT} + \eta_{nt}^{RT} \geq \frac{1}{2}\left(\overline{\lambda}_{nt}^{RT} - \underline{\lambda}_{nt}^{RT}\right)y_{nt}, \qquad \forall n\in N_L, \forall t>\tau \tag{17}$$

$$-y_{nt} \leq \left(E_{nt} - E_{nt}^{DA}\right) \leq y_{nt}, \qquad \forall n\in N_L, \forall t>\tau \tag{18}$$

$$\pi_{n\tau}, Z_n^{RT}, \eta_{nt}^{RT}, y_{nt} \geq 0.$$

The objective function has two parts, cost of the current hour τ and the cost of all future hours $t>\tau$. For all load nodes (N_L), the first part accounts for the current hour cost of energy purchased in the DA and RT markets, where the RT price $\lambda_{n\tau}^{RT} = \lambda_{n\tau}^{DA}|1+\varepsilon|$ is the known for the current hour and $E_{n\tau}$ is the actual consumption level (decided at the lower-level model).

For the future hours ($t>\tau$), since the RT prices are uncertain, the cost is assessed via a robust model similar to that presented in Refs. [38,39]. Let $\left[\overline{\lambda}_{nt}^{RT}, \underline{\lambda}_{nt}^{RT}\right]$ denote the RT price confidence bounds, which are obtained from simulated sample values drawn from $\lambda_{nt}^{DA}|1+\varepsilon|$. Using a robust parameters Γ_n^{RT}, the SO minimizes the worst-case total cost. The parameter Γ_n^{RT} can take any value within the interval $[0, |T-\tau|]$. When it is 0, then the risk of RT price uncertainty is ignored in all future hours, and hence the RT prices are taken as the mean values of the confidence bounds. When $\Gamma_n^{RT} = \left|T-\tau\right|$, in all future hours most conservative decisions are considered, the RT prices are taken as: the upper bounds when additional quantities are purchased in the RT market, and the lower bounds when the DA quantities are sold in the RT market. The terms Z_n^{RT} and η_{nt}^{RT} are the robust model decision variables. The constraint (16) determines the dynamic prices $\pi_{n\tau}$ for the current hour τ such that there is no revenue shortfall/surplus for the SO. Constraint (17) and (18) are from the strong duality theory of robust optimization model.

3.2.2. Lower-level model

This model is used by each aggregator (one for each load node $n\in N_L$) to optimally plan consumption among the current and the remaining hours of a day. It uses the binding dynamic prices for the current hour, decided at the upper level model. For the remaining hours, the model uses the DA prices as estimates of dynamic prices. As noted earlier, only the parking lot portion of the total load is scheduled by the aggregator. Each parking lot is considered to host a large number of EVs, that flow in and out at different hours of the day, and have different charging needs.

$$\min \pi_{n\tau}E_{n\tau} + \sum_{t=\tau+1}^{T}\lambda_{nt}^{DA}E_{nt}$$

s.t.

$$E_{nt} = P_{nt}^{r}\Delta t + \sum_{p=1}^{N_n^p}P_{nt}^{p}\Delta t, \quad (\rho_{nt}) \qquad \forall t\geq\tau \tag{19}$$

$$0 \leq P_{nt}^{p} \leq \overline{P}_{nt}^{p}, \quad \left(\underline{\mu}_{nt}^{p}, \overline{\mu}_{nt}^{p}\right) \qquad \forall t\geq\tau, \forall p\in N_n^{pl} \tag{20}$$

$$0 \leq SOC_{nt}^{p} \leq \overline{SOC}_{nt}^{p}, \quad (\underline{\nu}_{nt}^{p}, \overline{\nu}_{nt}^{p}) \qquad \forall t\geq\tau, \forall p\in N_n^{pl} \tag{21}$$

$$SOC_{nt}^{p} = SOC_{n(t-1)}^{p} + \eta_n^{p}P_{nt}^{p}\Delta t + \sum_{k\in C_n^{p}}\alpha_{nk}^{p}Q_{nk}^{p}T_{ntk}^{p} - \sum_{k\in C_n^{p}}\beta_{nk}^{p}Q_{nk}^{p}\widehat{T}_{ntk}^{p}, \quad (\psi_{nt}^{p}) \qquad \forall t\geq\tau, p\in N_n^{pl} \tag{22}$$

$$SOC_{nt}^{p} \geq \sum_{h\leq t}\sum_{k\in C_n^{p}}\alpha_{nk}^{p}Q_{nk}^{p}T_{nhk}^{p} - \sum_{h\leq t}\sum_{k\in C_n^{p}}\alpha_{nk}^{p}Q_{nk}^{p}\widehat{T}_{nhk}^{p}, \quad (\gamma_{nt}^{p}) \qquad \forall t\geq\tau, p\in N_n^{pl} \tag{23}$$

$$E_{nt}, P_{nt}^{p}, SOC_{nt}^{p} \geq 0$$

The first term of the objective function denotes the energy

consumption schedule for the current interval, and the second term accounts for the remaining hours. The constraint (19) ensures that the total load consumed is the sum of power consumed by fixed residential and business loads (P^r_{nt}) and the parking lots (P^p_{nt}), managed by the aggregator at node n in the time interval Δt, where N^{pl}_n is the number of parking lots at node n. Constraint (20) represents the maximum charging capacity of a parking lot, and constraint (21) ensures that the aggregate state of charge of a parking lot at any time t is not higher than the total capacity of the EVs present in the parking lot; the term $\overline{SOC}^p_{nt}$ is computed as $\sum_{h\le t}\sum_{k\in C^p_n} Q^p_{nk} T^p_{nhk} - \sum_{h\le t}\sum_{k\in C^p_n} Q^p_{nk} \widehat{T}^p_{nhk}$, where C^p_n is the maximum number of EVs in parking lot p and at node n, Q^p_{nk} is the battery capacity of vehicle k, and T^p_{ntk} and $\widehat{T}^p_{ntk}$ are binary variables for the time of arrival and the time of departure of the k^{th} EV. For instance, T^p_{ntk} value is 1, if k^{th} EV arrived at time t and 0 otherwise. Constraint (22) represents the state of charge at any time t, which is equal to the sum of: state of charge in the previous period $(t-1)$, power drawn from the grid for the parking lot in the interval Δt, and total state of charge of the vehicles arrived at time t, minus the total charge of the vehicles departed at time t. The coefficients η^p_n, α^p_{nk} and β^p_{nk} denote the conversion efficiency, percentage of charge at the time of arrival and departure, respectively. Constraint (23) ensures that the state of charge of the parking lot at any time t is at least equal to the sum of the initial state of charge of all parked EVs in the parking lot. The decision variables of the aggregator in this model are E_{nt}, P^p_{nt} and SOC^p_{nt} for all $t \ge \tau$. The dual variables associated with the constraints are given within the parentheses. We next formulate the KKT condition for the model. See Appendix A for the details.

3.2.3. Linearization of the upper-level model

The upper-level model has a nonlinear term $\pi_{n\tau}E_{n\tau}$ in (16). This nonlinearity is overcome by applying the strong duality principle on the lower-level model (see Section 3.2.2) as follows,

$$\pi_{n\tau}E_{n\tau} + \sum_{t=\tau+1}^{T} \lambda^{DA}_{nt} E_{nt} = \sum_{t\ge\tau}\left[P^r_{nt}\rho_{nt}\Delta t - \sum_{p=1}^{N^{pl}_n}\left\{ \overline{P}^p_{nt}\overline{\mu}^p_{nt} + \overline{SOC}^p_{nt}\overline{\nu}^p_{nt} - \left(\sum_{k\in C^p_n} \alpha^p_{nk} Q^p_{nk} T^p_{ntk} - \sum_{k\in C^p_n} \beta^p_{nk} Q^p_{nk} \widehat{T}^p_{ntk} \right) \psi^p_{nt} - \left(\sum_{h\le t}\sum_{k\in C^p_n} \alpha^p_{nk} Q^p_{nk} T^p_{nhk} - \sum_{h\le t}\sum_{k\in C^p_n} \alpha^p_{nk} Q^p_{nk} \widehat{T}^p_{nhk} \right) \gamma^p_{nt} \right\} \right] + SOC^p_{n(\tau-1)} \psi^p_{n\tau}. \tag{24}$$

Note from the above that, for the strong duality components corresponding to $\psi^p_{n\tau}$ (from (22) in Section 3.2.2), we have added an additional term $SOC^p_{n(\tau-1)}\psi^p_{n\tau}$ at the end of the equation. This is to account for the time $t = \tau$ when $SOC^p_{n(\tau-1)}$ will be a constant (which otherwise is a variable for all $t > \tau$). Also, at $\tau = 1, SOC^p_{n(\tau-1)}$ is zero.

3.2.4. The single level linear model

The following formulation represents the transformed bi-level model into a single-level linearized MPEC model, where constraint (16) is linearized using (24).

$$\min \sum_{n\in N_L}\left[\lambda^{DA}_{n\tau} E^{DA}_{n\tau} + \lambda^{RT}_{n\tau}\left(E_{n\tau} - E^{DA}_{n\tau}\right) + \sum_{t>\tau}^{T}\left(\lambda^{DA}_{nt} E^{DA}_{nt} + \frac{1}{2}\left(\overline{\lambda}^{RT}_{nt} + \underline{\lambda}^{RT}_{nt}\right)\left(E_{nt} - E^{DA}_{nt}\right)\right) + \Gamma^{RT}_n Z^{RT}_n + \sum_{t>\tau}^{T}\eta^{RT}_t \right]$$

s.t.

$$\sum_{t\ge\tau}\left[P^r_{nt}\rho_{nt}\Delta t - \sum_{p=1}^{N^{pl}_n} \overline{P}^p_{nt}\overline{\mu}^p_{nt} + \overline{SOC}^p_{nt}\overline{\nu}^p_{nt} - \left(\sum_{k\in C^p_n} \alpha^p_{nk} Q^p_{nk} T^p_{ntk} - \sum_{k\in C^p_n} \beta^p_{nk} Q^p_{nk} \widehat{T}^p_{ntk} \right) \psi^p_{nt} - \left(\sum_{h\le t}\sum_{k\in C^p_n} \alpha^p_{nk} Q^p_{nk} T^p_{nhk} - \sum_{h\le t}\sum_{k\in C^p_n} \alpha^p_{nk} Q^p_{nk} \widehat{T}^p_{nhk} \right) \gamma^p_{nt} \right] + SOC^p_{n(\tau-1)}\psi^p_{n\tau} - \sum_{t=\tau+1}^{T} \lambda^{DA}_{nt} E_{nt} - \lambda^{DA}_{n\tau} E^{DA}_{n\tau} - \lambda^{RT}_{n\tau}\left(E_{n\tau} - E^{DA}_{n\tau}\right) \ge 0, \quad \forall n \in N_L \tag{25}$$

Constraints (17) - (23) and (A.1) - (A.10),

$$\pi_{n\tau}, Z^{RT}_n, \eta^{RT}_{nt}, y_{nt}, E_{nt}, P^p_{nt}, SOC^p_{nt}, \rho_{nt}, \underline{\mu}^p_{nt}, \overline{\mu}^p_{nt}, \underline{\nu}^p_{nt}, \overline{\nu}^p_{nt}, \gamma^p_{nt} \ge 0,$$

ψ^p_{nt} – free variable.

4. Numerical results

We constructed a modified PJM 5-bus network in which the two load nodes are managed by aggregators. The loads consist of residential and business loads as well as large EV parking lots. The residential and business loads are assumed fixed, and only the parking lot loads are managed for demand response. We first give the network parameters, and then discuss implementation of our model on the network. Thereafter, we present a comparison of the total cost of meeting demands for policies derived from our model with other existing practices. The numerical experiments are carried out using Julia with Gurobi 7.0.1 solver on an Intel core i7 processor with 16 GB RAM.

4.1. Modified PJM 5-bus network

The network comprises three generating nodes with three generators in each, two load nodes, and six transmission lines (Fig. 2). Generator cost functions are quadratic and are obtained from Ref. [37]. The maximum limit of each generator is considered to be 800 MW. Demand at the two load nodes are constructed using 100 days of actual historical hourly demand data from two of the PJM zones DAY and AE for the year 2017 [40]. For computational simplicity, we first reduce the 100 demand patterns of each node into a small set of (five) representative dominant patterns with corresponding probabilities using the technique in Ref. [41]. The demand patterns are depicted in Fig. 3. We then calculate the average hourly demand of these five patterns, and considered 90 (85)% of the average hourly loads as the fixed loads for node 2 (node 3) and the rest as the EV load. Each of these patterns is considered as a demand scenario (ω) in the top-layer model. In the absence of historical data, demand at nodes can be forecasted based on socio-economic factors using methods discussed in Ref. [42]. The line connecting nodes 1 and 5 is considered to have a limited transmission capacity of 300 MW. The line reactances are as marked on

Fig. 2.

Aggregators at nodes 2 and 3 are each considered to manage 100 identical EV parking lots with the following characteristics. Each has a capacity of 1000 cars, of which 300 can be charged simultaneously. Each parking space has a charging rate of 11.5 kW (240 V, 48 A) with conversion efficiency (η_m^2) of 95%. Composition of the EVs is considered to be 60% Tesla Model S, 30% Nissan Leaf, and 10% Chevy Volt with battery capacities of 70 kWh, 40 kWh, and 18.4 kWh, respectively. The EVs are considered to arrive at the parking lots all hours of the day, with higher rates in the morning hours. EVs are considered to stay parked for at least 5 h, and depart at higher rates in the evening hours. The departure times of the vehicle in the lot are assumed known. Fig. 4 depicts simulated arrival and departure patterns of EVs in node 2. Similar patterns are generated for node 3. EVs are assumed to arrive at the parking lots with 20–40% charge, and leave with full charge. Charging of EVs require reactive power, which can cause an under voltage problem in the network. Hence, we have supplemented our DCOPF model with a constraint on the maximum number of vehicles that can be charged simultaneously (as stated before) to keep the reactive power consumption within a desirable level.

Before presenting the numerical results, we provide a brief step-by-step methodology for implementation of our two-layer model.

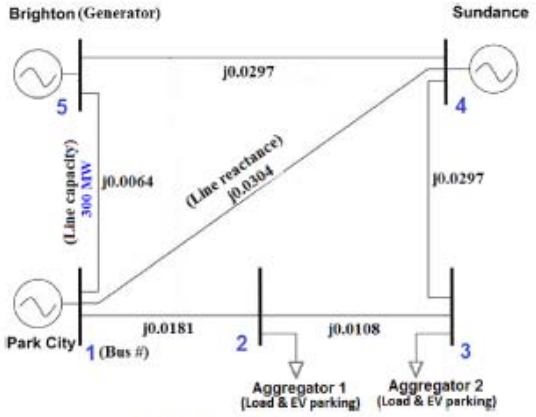

Fig. 2. Modified 5-bus PJM network.

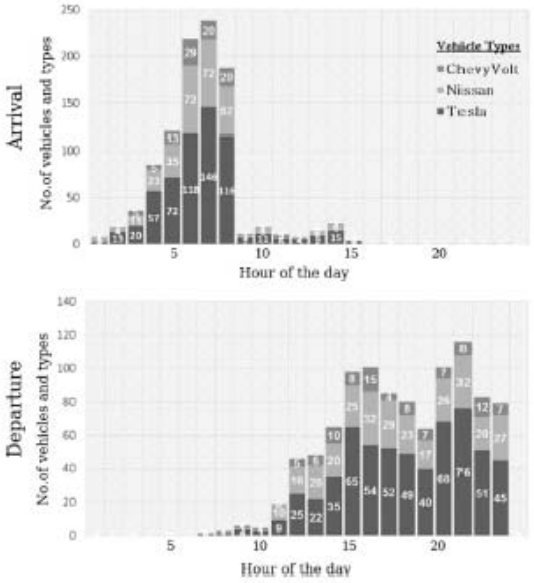

Fig. 4. Arrival and departure times of EVs of a parking lot at node 2.

- **Step 0:** The historical hourly demand data of each node is reduced to a set of dominant patterns (scenarios), product of which generates the total number of possible scenarios Ω. For each scenarios ($\omega \in \Omega$), we derive RT prices at each node and for all time periods. These demand patterns and corresponding RT prices serve as inputs for the top-layer model.
- **Step 1:** Using DA generators' supply bids, demand patterns and corresponding RT prices, the SO clears the DA market by solving the two-stage stochastic program that incorporates all network constraints. The solution of top-layer yields scheduled DA hourly quantities and corresponding DA prices, which are sent as input to the bottom layer.
- **Step 2:** The upper level of the bilevel model is solved by the SO to determine dynamic prices. The lower level model solves, for each aggregator, its energy consumption strategy. The bilevel model is reformulated as a single level MPEC model, which is further

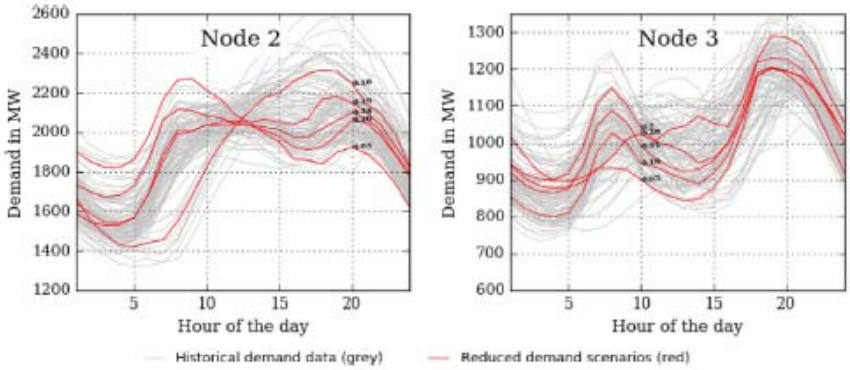

Fig. 3. Hourly demand scenarios for load at nodes 2 and 3.

linearized using strong duality principle. This converts the bilevel model into a single level MILP model.

4.2. Results from the top-layer model: DA market

The DA hourly quantities and prices for each load node are obtained from the two-stage stochastic program. For each demand scenario (ω) we derive RT prices, as discussed in Section 3.1. For which, the values for the parameters of the normal and Cauchy distributions are used as $(0, 0.1)$ and $(0.25, 0.05)$, respectively. The price spike probabilities (p_s) for different hours of the day at both load nodes are: $p_s = 0$ for hours 1–4 and 22–24; $p_s = 0.1$ for hours 5–12 and 19–21; $p_s = 0.25$ for hours 13–18. Note that, $p_s = k$ for an hour indicates that the RT price in that hour experiences spikes with a probability k.

Fig. 5 shows the DA quantities (in blue) in nodes 2 and 3 resulting from the top-layer two-stage stochastic model. The area shaded in grey represents the fixed residential and business loads, and the curves in red represent the demand scenarios. It may be observed that during the hours of no price spikes (e.g., hours 1–4 and 22–24), the DA scheduled quantities are close to the lowest demand scenario. This indicates that without the risk of price spikes, it is optimal to schedule less in DA market and procure any additional quantities during the actual hour in the RT market. On the other hand, when risk of price spike is higher the solution recommends higher DA quantities close to the highest demand scenario (e.g., hours 13–18). The numbers marked on the DA quantity curves in Fig. 5 are the hourly LMPs in $/MWh, which are sent as input to the bottom-layer model.

In this paragraph, using Fig. 6, we demonstrate how the RT price spikes can be adjusted in our model to represent various real scenarios. As shown in the box plots on top, for each value of p_s, from 0.1 to 0.9, we generated 30 samples of the RT prices considering a low value of the Cauchy distribution $\mu_2 = 0.25$ and MCP of $100/MWh. The box plots show the ratios of the RT price to MCP. Note that, for a low value of $p_s = 0.1$, the median of the ratio is close to one. The median rises to 1.3 for $p_s = 0.9$. The dots in the figure indicate the presence of sporadic larger spikes. This is similar to the average daily spikes encountered in ERCOT, NYSO, and CAISO markets. However, for higher values of the Cauchy distribution parameter μ_2, as shown in the bottom set of box plots, the price spike value increases, reaching to as high as six times higher than the MCP when $\mu_2 = 5.0$. Hence, by suitably selecting the parameters p_s and μ_2, our model can mimic price spike scenarios with different frequency of occurrence and magnitude.

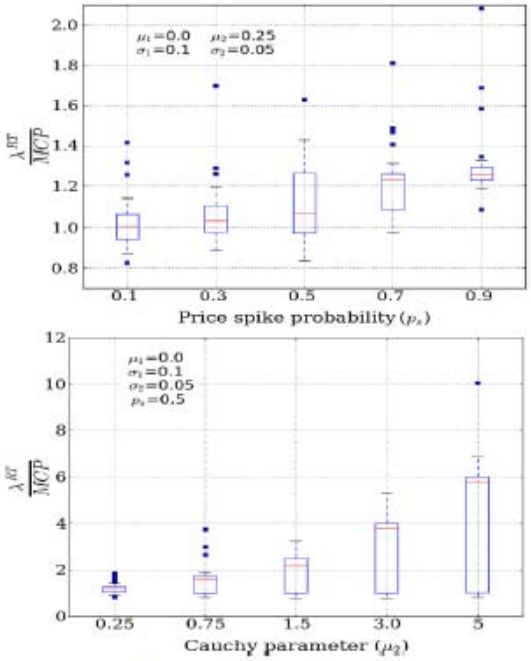

Fig. 6. RT price spikes for different p_s and μ_2.

4.3. Results from bottom-layer model: dynamic prices and EV charging schedules

Table 1 exhibits the bilevel model output for all 24 h for aggregator at node 2. These results are obtained using robust parameter (Γ_n^{RT}) value as 30%, and confidence bounds for future RT prices $\left[\underline{\lambda}_{nt}^{RT}, \overline{\lambda}_{nt}^{RT}\right]$ as 10% and 90%. We make several key observations from Table 1 using the rows in bold fonts.

It can be seen for hour 1 that the DA procured quantity is 1664.15 MW at a DA price of $93.3/MWh, while the actual total consumption is 1498.21 MW and the RT price of $113.53/MWh. As

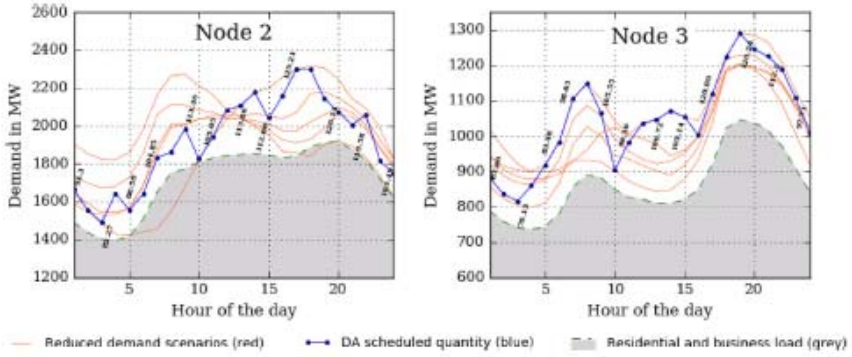

Fig. 5. DA scheduled quantities and corresponding prices at nodes 2 and 3.

Table 1
Load aggregator at node 2.

Time	DA Quantity (MW)	DA Price ($/MWh)	Dynamic price ($/MWh)	Total Demand (MW)	EV consumption (MW)	Resi. Demand (MW)	RT Price ($/MWh)	$\overline{\lambda}^{RT}$ ($/MWh)	$\underline{\lambda}^{RT}$ ($/MWh)	p_s
1	**1664.15**	**93.3**	**91.05**	**1498.21**	**9.2**	**1489.01**	**113.53**	**109.38**	**82.94**	**0**
2	1555.11	87.56	86.98	1466.16	29.9	1436.26	97.27	106.05	80.16	0
3	1490.51	82.27	82.3	1472.88	71.3	1401.58	79.92	104.08	78.66	0
4	**1642.6**	**91.99**	**92.28**	**1563.55**	**169.05**	**1394.5**	**86.4**	**105.22**	**78.69**	**0**
5	1557.34	88.58	88.58	1725.22	307.05	1418.18	88.58	110.28	76.67	0.1
6	1641.01	94.65	94.24	1855.67	345	1510.67	91.12	116.94	81.34	0.1
7	**1831.76**	**104.85**	**103.33**	**1999.39**	**345**	**1654.39**	**86.78**	**130.54**	**87.62**	**0.1**
8	**1862.7**	**107.39**	**106.66**	**1750.75**	**0**	**1750.75**	**118.78**	**135.44**	**90.74**	**0.1**
9	1985.29	113.36	113.36	2095.62	321.81	1773.81	113.36	131.04	94.09	0.1
10	1825.39	107.29	107.29	2154.85	345	1809.85	107.29	134.72	95.2	0.1
11	1943	105.09	105.72	2174.77	345	1829.77	111.04	130.23	95.96	0.1
12	2086	112.55	112.55	2059.56	216.98	1842.58	112.52	130.17	96.06	0.1
13	2106.64	113.86	113.62	2192.86	345	1847.86	107.75	140.77	97	0.25
14	2177	116.65	115.07	1855.25	0	1855.25	125.74	137.67	96.52	0.25
15	2041.95	112.08	107.64	1845.2	0	1845.2	153.72	139.43	95.4	0.25
16	2157.47	116.38	112.42	1830.31	0	1830.31	138.54	140.62	94.79	0.25
17	2299	129.21	129.18	1842.7	0	1842.7	129.32	142.88	97.36	0.25
18	2302.44	140.59	137.37	1887.11	0	1887.11	155.22	154.04	102.38	0.25
19	**2146.26**	**128.14**	**128.63**	**2242.1**	**331.33**	**1910.76**	**139.64**	**143.03**	**103.71**	**0.1**
20	2074.99	131	130.31	2261.82	345	1916.82	122.62	144.85	105.94	0.1
21	2005.33	119.58	117.44	2194.36	319.7	1874.66	94.79	138.48	103	0.1
22	2059.31	118.19	117.88	1991.72	171.84	1819.88	127.13	129.83	98.82	0
23	1817.92	103.49	103.48	1812.01	90.85	1721.16	106.47	123.09	93.68	0
24	1746.14	100.6	98.74	1621.47	0	1621.47	124.81	115.35	87.92	0

the RT price spike probability at this time is zero, the DA market schedules a quantity close to the lowest demand scenario. However, even without the spike, the basic variations in the RT price (modeled by normal distribution) has yielded a relatively high RT price of $113.53. As a result, the model chose to consume less than DA quantity and sell remaining in the RT market at a higher RT price. To balance this excess revenue, the revenue neutral SO offers a dynamic price ($91.05) that is lower than DA price ($93.3). Similar observations can be made for hour 8. Even with the presence of a significant number of EVs in the parking lots, optimal decision is not to charge any vehicles and keep the total demand low. At hour 4, the DA quantity is 1642.6 MW at a DA price of $91.99/MWh and RT price is $86.4/MWh. Though the RT price is lower, at hour 4, as the EV charging demand is low, the total demand is lower than the DA quantity. The excess DA amount is traded in the market at the RT price that is lower than DA price. To recover this loss, the revenue neutral SO selects a dynamic price that is higher than DA price. At hour 7, the DA quantity is 1831.76 MW at a DA price of $104.85/MW. The RT price $86.78/MWh is much lower than the DA price (as in hour 4). However, in contrast to hour 4, hour 7 has sufficient demand in the network to consume all of DA scheduled quantity and more. Hence, the SO offers a dynamic price ($103.33) that is lower than the DA price to promote consumption above the DA quantity. A final observation that we make is about time periods 8 and 19. At hour 8, the RT price is $118.78/MWh and the EV consumption is zero, whereas at hour 19, with RT price as $139.64/MWh and the EV consumption is very high (331.33 MW). This difference can be attributed to the vehicle charging needs close to departure times as well as the decisions the model made in previous hours 14–18 not to charge any EVs due to high RT prices.

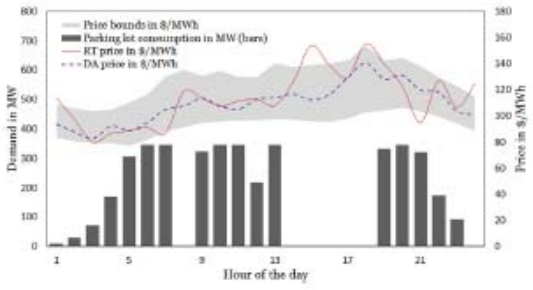

Fig. 7. Visualization of some results from Table 1.

For ease of further exposition of the numbers in Table 1, we develop combined plot of five of the columns from Table 1: DA price, RT price, lower and upper price bounds, and the total EV consumption (see Fig. 7). It depicts the trajectories of the DA and RT prices as well as the total hourly EV consumption. It may be noted that EV charging is avoided, when possible, during times of price spikes.

Results similar to those for node 2 are also observed for load at node 3. The daily average dynamic price for aggregators at nodes 2 and 3 are $109.45/MWh and $102.90/MWh, respectively. This difference can in part be attributed to the congestion in the network. Hereafter, we examine separately the impact of demand response and pricing practices on the daily cost to the consumers.

4.4. Impact of demand response and pricing practice

Here, we first examine the impact of demand response via optimal charging of EVs on the network. This is done by comparing the total cost to consumers under optimal charging with the cost of an adhoc EV charging strategy with no demand response. Those costs are assessed under the same dynamic pricing policy of our model. The comparison is replicated four times. For the optimal charging strategy, the solution is obtained for three different values of the robust parameter Γ_n^{RT} (0, 0.3, and 0.5). The comparison results for load node 2 are presented in Table 2. In all four replicates, the total cost of meeting the demands under optimal EV charging strategy is lower than the adhoc strategy. Based on the average values shown in the last row, the overall average dynamic price with demand response is $1.4/MWh lower than that of dynamic price with no demand response (adhoc policy). Also, the total

Table 2
Optimal policy vs adhoc policy for load at node 2.

Optimal policy						Adhoc policy	
$\Gamma_n^{RT} = 0$		$\Gamma_n^{RT} = 0.3$		$\Gamma_n^{RT} = 0.5$			
Total cost	Avg.DP ($/MWh)	Total cost	Avg.DP ($/MWh)	Total cost	Avg.DP ($/MWh)	Total cost	Avg.DP ($/MWh)
$4,996,992	110.08	$4,994,972	110.04	$5,007,262	110.31	$5,047,213	111.19
$4,961,292	109.30	$4,968,471	109.45	$4,987,796	109.88	$5,022,622	110.65
$4,966,925	109.42	$4,943,053	108.89	$4,941,478	108.86	$5,063,857	111.55
$5,156,280	113.59	$5,159,984	113.67	$5,167,509	113.84	$5,217,924	114.95
$5,020,372	**110.60**	**$5,016,620**	**110.51**	**$5,026,011**	**110.72**	**$5,087,904**	**112.08**

consumer cost saving from demand response is $70,000 per day. Similar results are observed for load node 3, which yield a reduction in the daily average dynamic price of $1.8/MWh and the daily cost saving of $45,000. Hence, the total consumer cost saving obtain via demand response for nodes 2 and 3 (with EV parking lots representing 10% and 15% of the total loads) for the sample 5-bus network is $115,000 per day and $42 million per year.

We now compare the benefits of our dynamic pricing strategy with those obtained from the commonly used pricing practices: flat pricing, TOU pricing, and CPP. We present the comparison for load node 3 (See Table 3). For the flat pricing policy, we consider the average of the 24 hourly DA prices at node 3 (from the top-layer model) as the fixed price throughout the day, which is obtained as $102.58/MWh. For TOU pricing, we assume that flat price of $102.58/MWh prevails for all hours except the peak hours 13–18 when the price is 1% higher ($103.61). For CPP, we consider the same flat price except for the hours when the RT price exceeds the flat price by 20%, at those times the price increases by 1%.

Table 3 exhibits the results for daily average price ($/MWh), cost to the consumers, and revenue of SO for all the above pricing practices. Also given within parenthesis (in bold) are the effective cost to the consumers for each pricing practice. The effective costs are used for fair comparison and are obtained by passing the SO's revenue shortfall/surplus to the consumers cost. The dynamic pricing policy, implemented with Γ_n^{RT} as 30%, results in a daily average price of $101.85/MWh (less than the flat price) with a total consumer cost of $2,529,117 and SO revenue of $21 (approximately revenue neutral). For flat pricing policy, the total daily effective cost to consumers is $36,584 higher than the dynamic pricing policy. The SO experiences a revenue loss of $18,388 in TOU. We examined two other adhoc flat pricing scenarios with prices 1% higher (row 2) and 1% lower (row 3) than the fixed price of $102.58/MWh. In the case of 1% higher price, which is motivated by the desire to avoid SO revenue loss, the effective cost to consumer remains the same while the SO revenue swings to a surplus of $7190. When flat price is reduced by 1%, the SO revenue loss soars to $43,716. For TOU pricing policy, the effective cost to consumers is higher by $10,897 than the dynamic policy. As in the case of flat pricing, we examine two other TOU scenarios with flat prices 1% higher and lower. For CPP, the effective cost to consumer is $2418 higher than the dynamic pricing. As in flat and TOU policies, outcomes for the two other CPP scenarios are not as desirable as the revenue neutral dynamic pricing policy. The effective cost to consumers decreases in the pricing sequence: flat, TOU, CPP and dynamic. Similar observations are also obtained for load node 2.

5. Concluding remarks

We have developed a robust game-theoretic model that simultaneously yields hourly binding dynamic prices of electricity (for SO) and the corresponding demand response actions using EVs (for load aggregators). The model aims to minimize the cost to consumers in a network subjected to price spikes, and keep the SO revenue neutral. Our model is formulated as a two-layer optimization model where the top-layer is a two-stage stochastic model and the bottom-layer is a bilevel model. We have demonstrated the implementation of the model on a modified 5-bus PJM network in which 10–15% of the total load is consumed by EVs that participate in DR; thermostatic loads are not considered as part of DR. A low to moderate price spike scenario where the median price is 1.25–1.5 times higher than the base price is examined. It is shown that by using dynamic pricing and demand response, the daily average consumer cost is 1.5% lower than the cost when dynamic pricing is offered but no demand response actions are taken. The consumer cost resulting from the use of our dynamic pricing and demand response policy is also compared with the cost from the flat pricing policy, for which we achieve a reduction of 1.42%. We also implemented our model on a high price spikes scenario with a median price spike 3.5 times higher than the base price. For this, we achieve a daily average consumer cost reduction of 6.5% from flat pricing. It is evident that our model is able to accommodate price spikes and yield appropriate policy for dynamic pricing and demand response to support SOs and load aggregators. The above mentioned benefits of our model are quite as expected, as researchers and practitioners have long predicted that a true form of dynamic pricing and network wide demand response will bring such benefits. A recent paper claimed the expected cost benefits to be between 2 and 4% [6].

Table 3
Comparison of dynamic pricing with traditional pricing for load at node 3.

Dynamic pricing			Flat Pricing			TOU pricing			CPP		
Avg $/MWh	Total cost ($)	SO Revenue ($)	Avg $/MWh	Total cost ($)	SO Revenue ($)	Avg $/MWh	Total cost ($)	SO Revenue ($)	Avg $/MWh	Total cost ($)	SO Revenue ($)
101.85	2,529,117 **(2,529,096)**	21	102.58	2,547,292 **(2,565,680)**	−18,388	102.58, 103.61	2,552,681 **(2,539,993)**	12,688	102.58, 103.61	2,551,021 **(2,531,514)**	19,508
			103.61	2,572,869	7190	103.61, 104.64	2,578,258	38,265	103.61, 104.64	2,576,599	46,818
			101.56	2,521,963	−43,716	101.56, 102.57	2,527,247	−12,746	101.56, 102.57	2,526,653	−3699

We note that, application of our model in real networks with many buses will introduce a number of computational challenges. For example, in the top-layer model the total number of demand scenarios (Ω) will increase exponentially with the number of load buses. The constraint matrix of the network, in the top-layer model, will also grow large and sparse. Use of efficient scenario reduction techniques (as in Ref. [41]) and inherent capability of Gurobi optimizer to deal with sparse matrices can be used to alleviate some of the above challenges. As far as the bottom layer model is concerned, the number of EV aggregator models that we need to solve in the lower level will increase linearly with the number of load buses. Since these models are considered to be independent of each other, a distributed computational approach can address this. Implementation of our model for a large network therefore is a topic of future research.

Appendix A. KKT formulation for the lower-level (aggregator's) model

In order to convert the bilevel model of the bottom-layer into a single level mixed integer programming model, we write the KKT conditions for each load node in the lower-level. The KKT conditions comprise the set of stationarity conditions (A.1)-(A.5) with respect to dual variables of the aggregator's problem, complementary slackness conditions (A.6)-(A.10), and collection of constraints (19)-(23). The KKT conditions for a load node $n \in N_L$ are given as follows.

$$\rho_{n\tau} \leq \pi_{n\tau}, \quad (E_{n\tau}) \tag{A.1}$$

$$\rho_{nt} \leq \lambda_{nt}^{DA}, \quad (E_{nt}) \qquad \forall t > \tau \tag{A.2}$$

$$-\rho_{nt}\Delta t + \underline{\mu}_{nt}^{p} - \overline{\mu}_{nt}^{p} - \eta_n^p \psi_{nt}^{p} \Delta t \leq 0, \quad (P_{nt}^{p}) \qquad \forall t \geq \tau, \forall p \in N_n^{pl} \tag{A.3}$$

$$\underline{\nu}_{nt}^{p} - \overline{\nu}_{nt}^{p} + \psi_{nt}^{p} - \psi_{n(t+1)}^{p} + \gamma_{nt}^{p} \leq 0, \quad (SOC_{nt}^{p}) \quad \forall t = \tau, \cdots, T-1, \forall p \in N_n^{pl} \tag{A.4}$$

$$\underline{\nu}_{nt}^{p} - \overline{\nu}_{nt}^{p} + \psi_{nt}^{p} + \gamma_{nt}^{p} \leq 0, \quad (SOC_{nt}^{p}) \qquad \forall t = T, \forall p \in N_n^{pl} \tag{A.5}$$

$$0 \leq \underline{\mu}_{nt}^{p} \perp P_{nt}^{p} \geq 0, \qquad \forall t \geq \tau, \forall p \in N_n^{pl} \tag{A.6}$$

$$0 \leq \overline{\mu}_{nt}^{p} \perp \left(\overline{P}_{nt}^{p} - P_{nt}^{p}\right) \geq 0, \qquad \forall t \geq \tau, \forall p \in N_n^{pl} \tag{A.7}$$

$$0 \leq \underline{\nu}_{nt}^{p} \perp SOC_{nt}^{p} \geq 0, \qquad \forall t \geq \tau, \forall p \in N_n^{pl} \tag{A.8}$$

$$0 \leq \overline{\nu}_{nt}^{p} \perp \left(\overline{SOC}_{nt}^{p} - SOC_{nt}^{p}\right) \geq 0, \forall t \geq \tau, \forall p \in N_n^{pl} \tag{A.9}$$

$$0 \leq \gamma_{nt}^{p} \perp \left[SOC_{nt}^{p} - \left(\sum_{h \leq t} \sum_{k \in C_n^p} \alpha_{nk}^{p} Q_{nk}^{p} T_{nhk}^{p} - \sum_{h \leq t} \sum_{k \in C_n^p} \alpha_{nk}^{p} Q_{nk}^{p} \widehat{T}_{nhk}^{p} \right) \right] \geq 0, \quad \forall t \geq \tau, \forall p \in N_n^{pl} \tag{A.10}$$

$\rho_{nt}, \underline{\mu}_{nt}^{p}, \overline{\mu}_{nt}^{p}, \underline{\nu}_{nt}^{p}, \overline{\nu}_{nt}^{p}, \gamma_{nt}^{p} \geq 0, \psi_{nt}^{p}$ – free variable.

Note that, the stationarity condition for the primal variable (E_{nt}) is split into two parts, for the current hour τ (A.1) and for all future hours $t > \tau$ (A.2). Similarly, for the primal variable SOC_{nt}^{p}, we have two inequalities, one for all $t < T$ (A.4) and the other for T (A.5), as there is no state update from T to $T+1$. The complementary slackness conditions (A.6)-(A.10) are of the general form $0 \leq u \perp h(x) \geq 0$, which are linearized by substituting with the following: $u \geq 0$, $h(x) \geq 0$, $u \leq Mz$ and $h(x) \leq M(1-z)$, where (big) M is a large constant and z is a 0–1 binary decision variable.

References

[1] Borenstein S, Jaske M, Rosenfeld A. Dynamic pricing, advanced metering, and demand response in electricity markets. UC Berkeley: Center for the Study of Energy Markets; 2002.
[2] Dutta G, Mitra K. A literature review on dynamic pricing of electricity. J Oper Res Soc 2017;68(10):1131–45.
[3] Khan AR, Mahmood A, Safdar A, Khan ZA, Khan NA. Load forecasting, dynamic pricing and dsm in smart grid: a review. Renew Sustain Energy Rev 2016;54:1311–22.
[4] Hu Z, Kim J-h, Wang J, Byrne J. Review of dynamic pricing programs in the us and europe: status quo and policy recommendations. Renew Sustain Energy Rev 2015;42:743–51.
[5] Faruqui A, Hledik R, Newell S, Pfeifenberger H. The power of 5 percent. Electr J 2007;20(8):68–77.
[6] Faruqui A, Hajos A, Hledik R, Newell S. Fostering economic demand response in the Midwest ISO. Energy 2010;35(4):1544–52.
[7] LCG consulting, energy price, http://www.energyonline.com/, accessed: June, 12, 2018.
[8] Block D, Harrison J, Center FSE, Dunn MD. Electric vehicle sales and future projections, electric vehicle transportation center. University of Central Florida; 2014. Tech. Rep (1).
[9] Quillinan JD. Pricing for retail electricity. J Revenue Pricing Manag 2011;10(6):545–55.
[10] Kaluvala NS, Forman A. Smart grid. Int J E Polit 2013;4(2):39–47.
[11] Faruqui A, Sergici S, Akaba L. The impact of dynamic pricing on residential and small commercial and industrial usage: new experimental evidence from Connecticut. Energy J 2014:137–60.
[12] Faruqui A, Palmer J. The discovery of price responsiveness–a survey of experiments involving dynamic pricing of electricity. Brattle group; 2012.
[13] Ahmad F. The ethics of dynamic pricing. Electr J 2010;23:13–27.
[14] Borenstein S. Effective and equitable adoption of opt-in residential dynamic electricity pricing. Rev Ind Organ 2013;42(2):127–60.
[15] Ottesen SO, Tomasgard A, Fleten S-E. Prosumer bidding and scheduling in electricity markets. Energy 2016;94:828–43.
[16] Ottesen SO, Tomasgard A, Fleten S-E. Multi market bidding strategies for demand side flexibility aggregators in electricity markets. Energy 2018;149:120–34.
[17] Iria J, Soares F, Matos M. Optimal supply and demand bidding strategy for an aggregator of small prosumers. Appl Energy 2018;213:658–69.
[18] Gomez-Herrera JA, Anjos MF. Optimal collaborative demand-response planner for smart residential buildings. Energy 2018;161:370–80.
[19] Mohseni A, Mortazavi SS, Ghasemi A, Nahavandi A, et al. The application of household appliances' flexibility by set of sequential uninterruptible energy phases model in the day-ahead planning of a residential microgrid. Energy 2017;139:315–28.
[20] Subramanian V, Das TK, Kwon C, Gosavi A. Data-driven learning model for dynamic pricing and demand response in smart and connected communities. 2017. http://vigneshs.myweb.usf.edu/publications/index.html/. [Accessed 12 June 2018].
[21] Bessa RJ, Matos MA. Economic and technical management of an aggregation agent for electric vehicles: a literature survey. Int Trans Electr Energy Syst 2012;22(3):334–50.
[22] San Román TG, Momber I, Abbad MR, Miralles AS. Regulatory framework and business models for charging plug-in electric vehicles: infrastructure, agents, and commercial relationships. Energy Pol 2011;39(10):6360–75.
[23] Ortega-Vazquez MA, Bouffard F, Silva V. Electric vehicle aggregator/system operator coordination for charging scheduling and services procurement. IEEE Trans Power Syst 2013;28(2):1806–15.
[24] Vayá MG, Andersson G. Optimal bidding strategy of a plug-in electric vehicle aggregator in day-ahead electricity markets under uncertainty. IEEE Trans Power Syst 2015;30(5):2375–85.
[25] Shafie-Khah M, Heydarian-Forushani E, Golshan M, Siano P, Moghaddam M, Sheikh-El-Eslami M, Catalão J. Optimal trading of plug-in electric vehicle aggregation agents in a market environment for sustainability. Appl Energy 2016;162:601–12.
[26] Momber I, Siddiqui A, San Román TG, Söder L. Risk averse scheduling by a PEV aggregator under uncertainty. IEEE Trans Power Syst 2015;30(2):882–91.
[27] Alipour M, Mohammadi-Ivatloo B, Moradi-Dalvand M, Zare K. Stochastic scheduling of aggregators of plug-in electric vehicles for participation in energy and ancillary service markets. Energy 2017;118:1168–79.
[28] Nezamoddini N, Wang Y. Risk management and participation planning of electric vehicles in smart grids for demand response. Energy 2016;116:

836–50.
[29] Aghajani S, Kalantar M. A cooperative game theoretic analysis of electric vehicles parking lot in smart grid. Energy 2017;137:129–39.
[30] Li J, Li C, Xu Y, Dong Z, Wong K, Huang T. Noncooperative game-based distributed charging control for plug-in electric vehicles in distribution networks. IEEE Trans Ind Inf 2018;14:301–10.
[31] Xi X, Sioshansi R. Using price-based signals to control plug-in electric vehicle fleet charging. IEEE Trans Smart Grid 2014;5(3):1451–64.
[32] Aghajani S, Kalantar M. Operational scheduling of electric vehicles parking lot integrated with renewable generation based on bilevel programming approach. Energy 2017;139:422–32.
[33] Neyestani N, Damavandi MY, Shafie-Khah M, Bakirtzis AG, Catalão JP. Plug-in electric vehicles parking lot equilibria with energy and reserve markets. IEEE Trans Power Syst 2017;32(3):2001–16.
[34] Zhou C, Qian K, Allan M, Zhou W. Modeling of the cost of ev battery wear due to v2g application in power systems. IEEE Trans Energy Convers 2011;26(4):1041–50.
[35] Wang Q, Yang F, Wang S, Liu Y-H. Bilevel programs with multiple followers. Syst Sci Math Sci 2000;13.
[36] Dempe S, Dutta J. Is bilevel programming a special case of a mathematical program with complementarity constraints? Math Program 2012;131(1–2):37–48.
[37] Das D, Wollenberg BF. Risk assessment of generators bidding in day-ahead market. IEEE Trans Power Syst 2005;20(1):416–24.
[38] Bertsimas D, Sim M. Robust discrete optimization and network flows. Math Program 2003;98(1–3):49–71.
[39] Rahimiyan M, Baringo L. Strategic bidding for a virtual power plant in the day-ahead and real-time markets: a price-taker robust optimization approach. IEEE Trans Power Syst 2016;31(4):2676–87.
[40] ISO PJM, LLS., https://www.pjm.com/, accessed: June, 12, 2018.
[41] Growe-Kuska N, Heitsch H, Romisch W. Scenario reduction and scenario tree construction for power management problems. In: Power tech conference proceedings, vol. 3. IEEE Bologna; 2003. p. 7. IEEE, 2003.
[42] Kaboli SHA, Selvaraj J, Rahim N. Long-term electric energy consumption forecasting via artificial cooperative search algorithm. Energy 2016;115:857–71.

Appendix E: Published Material in IEEE PES General Meeting

Controlled Islanding of Power Networks based on Anticipated Severity of Extreme Events

Vignesh Subramanian, Tapas K. Das, and Hadi Charkhgard
Department of Industrial and Management Systems Engineering,
University of South Florida,
Tampa, FL, 33620 USA

***Abstract*—A new mixed integer programming model is presented for developing islanding strategies for power grids when disruptions from extreme events are anticipated. It minimizes the total cost arising from planned load reduction together with the cost of unplanned load loss and network recovery. The later cost is a function of the severity of the anticipated extreme event. The model selects an appropriate number of islands and their sizes depending on the severity, Islanding results for IEEE 30-bus test system is presented.**

***Index Terms*—Islanding, extreme event, load shedding, resilience, graph-partitioning, mixed integer programming**

I. Introduction

Extreme weather events such as hurricanes and storms routinely put millions of energy consumers in the dark by disrupting transmission and distribution lines in the power grid infrastructure. It was reported in [1] that 80% of major power outages that happened in the U.S. between 2003 - 2012 were caused by weather events, and on average about 15 million consumers were affected each year. These extreme weather events are known to be low frequency high impact phenomenon that pose severe threat to the grid. Also, it is believed [2] that the evolving change in climate will likely cause more severe weather events with higher frequency causing greater disruptions in future. Since our dependence on the power grid has grown dramatically and is going to increase even further (e.g., electric vehicles), it is paramount that we develop better means of avoiding system wide failures and make the power grid more resilient. Utility regulators have introduced the notion of grid resiliency as *robustness and recovery characteristics of utility infrastructure and operations, which avoid or minimize interruptions of service during an extraordinary and hazardous event [3].*

The power grids in recent years have begun a revolutionary change with the rise of smart grids supported by new communication and IoT technologies. This transformation has facilitated in better grid operations and control during moderated disruptions. However, responding to extreme events to improve resilience is still a challenge. To address this, we must improve the system flexibility [4] and connectivity [5]. Flexibility addresses the system adaptation for changing conditions brought on by extreme events, and connectivity provides a wide spread situation awareness about the grid. The combination of both can help system operators to make decisions when a grid is under threat. Measures to harden the power grid against extreme weather events for resilience [6] are classified as short term and long term. Short term measures refer to preventive and corrective actions before, during, and after an event. Long term measures address preparedness for future events. Our focus in this paper is on a particular short term measure, viz., grid islanding before an event (e.g., severe storms).

During severe storms, power grids undergo unplanned islanding by dynamically responding to the line outages in order to prevent cascading failures. Islanding refers to reconfiguration of an interconnected grid into multiple isolated subnetworks. Unplanned islanding may not be timely to prevent cascading and may also lead to problems like voltage and frequency instabilities. Hence, planned islanding considering optimal utilization of generating and other resources is essential for resilience. Islanding approaches must also consider minimizing the effects of total load shedding in the overall grid.

The contribution of this paper includes a mixed integer programming (MIP) formulation of the intentional islanding approach. The model aims to minimize the total cost of islanding comprising the cost of planned load reduction and the cost of unplanned load loss and network recovery as a function of the severity of the event. The MIP model subsumes the DC power flow model to account for generation and transmission related constraints. It also assures full connectivity among the buses within the islands.

We adopted a graph-theoretical approach in which the interconnected power network is represented by a graph with vertices as buses and edges as transmission lines. Hence, the islanding process is a graph partitioning problem integrated with the DC power flow model. Remainder of this paper is organized as follows. Section 2 discusses the existing literature on islanding. Section 3 outlines the major assumptions made for the model. The MIP formulation is presented in Section 4. The numerical results obtained by applying the MIP model for IEEE-30 bus test system are presented in Section 5. Section 6 presents the concluding remarks including the model limitations.

II. Related work

Early research on controlled islanding is based on grouping coherent generators in the system to deal with large disturbances [7], [8]. This islanding method is implemented

978-1-5386-7703-2/18/$31.00 ©2018 IEEE

as a corrective measure in response to disruption event(s). The method presented in [9] uses a combination of graph partitioning and grouping of coherent generators to collapse a set of nodes into a single dummy node. In [10], an ordered binary tree based splitting algorithm is proposed for large scale power networks. The models presented in [11]–[13] offer mixed integer programming formulations that, for a specified number of islands, determine the optimal grouping of buses to minimize the load shedding. These models do not consider the severity of the expected disruptions. In recent years, meta heuristics methods [14] and spectral clustering optimization [15] were suggested for islanding.

III. Assumptions

We made two major assumptions in our formulation. We considered that sufficient reactive power support is available to maintain voltage. This assumption is necessary, since the DC power flow model ensures active power balance only. Imbalance of reactive power results voltage instabilities, which could cause black-outs. We also assume that the generators that belong to an island are coherent. Hence, no specific constraint is incorporated in the model for generator coherency.

IV. MILP-based optimal islanding model

A. Notation

Indices

i	Index of bus/node
k	Index of Island

Sets

V	Set of buses
$(i,j) \in E$	Transmission line between buses i and j in set E
$(i,j),(j,i) \in D$	Directed links between buses i and j, if $(i,j) \in E$
G_i	Set of generators at bus i
A_i	Set of loads at bus i
T_i	Set of transmission lines incident on bus i

Variables

F_{ij}	Line flow in MW between buses i and j
P^G_{il}	Power (in MW) generated by the l^{th} conventional unit in bus i
δ_i	Load angle of a bus i in rad
r_{il}	Load curtailment (in MW) for the l^{th} load at bus i
S	Maximum size of Island in the network
x_{ik}	Binary variable to denote if bus i belongs to the k^{th} island
y_{ij}	Binary variable to denote whether buses i and j belong to same island and are connected by a line
w_O	Flow out of dummy node O to ensure network connectivity
σ	Variable used to ensure network connectivity
β, γ	Variables used in linearizing the non-linear terms in the constraints

Constants

α	Parameter designating severity of disruption
d_{il}	Demand (in MW) at l^{th} load at bus i
b_{ij}	Susceptance of a line connecting buses i and j
K	Upper bound for the number of possible islands considered by the model
$\overline{F}_{ij}$	Maximum power flow in line (i,j)
$\overline{P}^G_{il}, \underline{P}^G_{il}$	Maximum and minimum generation capacity in MW
$\overline{\delta}_i, \underline{\delta}_i$	Maximum and minimum load angle in rad
c_{il}	Unit cost of load curtailment
M	Arbitrary large number used by the big M method

B. Controlled Islanding Model

The objective function (1) minimizes the total cost and it has two parts. The first part accounts for the cost of planned load loss due to islanding. The second part assesses the total cost of unplanned load loss during the storm together with the cost network recovery. The latter cost depends on the severity of an event and is represented in the model by the parameter α (as a function of the number of buses in the largest island in the network). Note in the objective function that the maximum number of buses in the islands is kept small to limit the impact, the load shedding cost increases, and vice versa.

$$\min \sum_{i \in V} \sum_{l \in A_i} c_{il} r_{il} + \alpha S \quad (1)$$

s.t.

$$\sum_{l \in G_i} P^G_{il} - \sum_{j \in T_i} b_{ij}[\delta_i - \delta_j] y_{ij} - \sum_{l \in A_i} [d_{il} - r_{il}] = 0, \qquad \forall i \in V \quad (2)$$

$$-\overline{F}_{ij} \le b_{ij}[\delta_i - \delta_j] \le \overline{F}_{ij}, \qquad \forall i \in V, j \in T_i : j < i \quad (3)$$

$$\underline{P}^G_{il} \le P^G_{il} \le \overline{P}^G_{il}, \qquad \forall l \in G_i, \forall i \in V \quad (4)$$

$$\underline{\delta}_i \left(1 - \sum_{k=1}^{K} \sigma_i^k\right) \le \delta_i \le \overline{\delta}_i \left(1 - \sum_{k=1}^{K} \sigma_i^k\right), \qquad \forall i \in V \quad (5)$$

Islanding Constraints

$$\sum_{k=1}^{K} x_{ik} = 1, \qquad \forall i \in V \quad (6)$$

$$y_{ij} = \sum_{k=1}^{K} x_{ik} x_{jk}, \qquad \forall (i,j) \in E \quad (7)$$

$$S \ge \sum_{i \in V} x_{ik} + \sum_{i \in V} \sum_{k=1}^{K} \sigma_j^k, \qquad k = 1, \cdots, K \quad (8)$$

Network Connectivity

$$w^k_{Oj} = \left(\sum_{j'=1}^{|V|} x_{j'k}\right) \sigma_j^k, \qquad \forall j \in V, k = 1, \cdots, K \quad (9)$$

$$\sum_{j=1}^{|V|} \sigma_j^k \le 1, \qquad k = 1, \cdots, K \quad (10)$$

$$\sigma_j^k \le x_{jk} \qquad \forall j \in V, k = 1, \cdots, K \quad (11)$$

$$x_{jk} = \sum_{(i,j) \in D} w^k_{ij} - \sum_{(j,i) \in D} w^k_{ji} + w^k_{Oj}, \qquad \forall j \in V, k = 1, ..., K \quad (12)$$

$$0 \le w^k_{ij} \le |V| x_{jk}, \qquad \forall (i,j) \in D \quad (13)$$

$$0 \le w^k_{ij} \le |V| x_{ik}, \qquad \forall (i,j) \in D \quad (14)$$

$$x_{ik} \in \{0,1\}^{|V| \times K}, y_{ij} \in \{0,1\}^{|V| \times |V|},$$
$$r_{il} \in \{0,1\}^{|V| \times |A_i|}, \sigma_i^k \in \{0,1\}^{|V| \times K}$$

The constraint (2) is a modified DC power balance constraint, where the binary variable y_{ij} is used to check if the buses i and j belong to the same island as well as if they are directly connected. The value of this variable is guided by constraint (7). The inequality constraints (3)-(5) account for the bounds on the transmission line flows, power generation, and load angle limits on each bus, respectively. The significance of the term σ in constraint (5) is discussed

later. The constraint (6) ensures that a bus belongs to any one island only, and constraint (8) determines the maximum size of the islands (measured by the # of buses).

The network constraints (9) through (14) ensure that all the buses within each island are connected. These equations are adopted from the single commodity flow model reported in [16]. Per this approach, we invoke a dummy node O that acts as the source node and all other nodes of all islands are sink nodes. Each sink node is assumed to draw one unit of flow. The constraint (9) determines the outflow from the dummy node to one node in each island. These outflow are equal to the total number of nodes in respective islands. Constraint (10) helps in choosing the node to which the dummy node is connected. Constraints (10) and (5) together help to decide the reference bus (with load angle zero) for each island and also the other load angles at other buses within the limits. Constraint (12) helps to ensure that each bus consumes one unit of flow.

C. Constraint Linearization

The power balance constraint (2) has a nonlinear term $b_{ij}[\delta_i - \delta_j]y_{ij}$. It is linearized as follows (as in [17]).

$$\sum_{l\in G_i} P_{il}^G - \sum_{j\in T_i} F_{ij} - \sum_{l\in A_i} [d_{il} - r_{il}] = 0, \qquad \forall i \in V$$
$$-M(1-y_{ij}) \le F_{ij} - b_{ij}[\delta_i - \delta_j] \le M(1-y_{ij}), \quad \forall (i,j) \in E$$
$$-\overline{F}_{ij} y_{ij} \le F_{ij} \le \overline{F}_{ij} y_{ij}, \qquad \forall (i,j) \in E$$

Islanding constraints (7) is linearized as follows.

$$y_{ij} = \sum_{k=1}^{K} \gamma_{ikj}, \qquad \forall (i,j) \in E$$
$$\gamma_{ikj} \ge x_{ik} + x_{jk} - 1, \quad \forall i \in V, k = 1, \cdots, K, \forall j \in V$$
$$\gamma_{ikj} \le x_{ik}, \quad \forall i \in V, k = 1, \cdots, K, \forall j \in V$$
$$\gamma_{ikj} \le x_{jk}, \quad \forall i \in V, k = 1, \cdots, K, \forall j \in V$$

Network connectivity constraint (9) is linearized as follows.

$$w_{oj}^k = \sum_{j' \in V} \beta_{j'kj}, \qquad \forall j \in V, k = 1, \cdots, K$$
$$\beta_{j'kj} \ge x_{j'k} + \sigma_j^k - 1, \quad \forall j' \in V, k = 1, \cdots, K, j \in V$$
$$\beta_{j'kj} \le x_{j'k}, \quad \forall j' \in V, k = 1, \cdots, K, j \in V$$
$$\beta_{j'kj} \le \sigma_j^k, \quad \forall j' \in V, k = 1, \cdots, K, j \in V$$

V. Numerical Results

We implemented our severity (of extreme events) guided islanding model on the IEEE-30 bus network. We considered generators at buses 1, 2, 5, 8, 11, and 13 with maximum capacities of 100, 60, 80, 20, 10, and 15 MW, respectively. We maintained the load levels at all buses unaltered and considered only the reactance for the transmission lines. We substituted the transformers with transmission lines with same reactance. We considered a load reduction cost of \$10 per MW for all loads. Various levels of anticipated severity of the extreme events were examined using α values between 0 and 100, where 0 indicates no occurrence of extreme events and is used for benchmarking only. For each severity scenario, the model is solved for a number of reasonable upper bounds for the number of islands to consider. It can be seen from the results shown in Table I that the model decides the optimal number of islands for given upper bound and the level of severity. The results show that for any given upper bound (say, 4), as the severity increases, the model recommends increasing numbers of islands as follows. In the absence of extreme events ($\alpha = 0$), no islanding is recommended, as expected, and all 30 buses are interconnected. For $\alpha = 30$, the model recommends two islands with 12 and 18 buses. For the severity levels of 50 and 70, the model recommends identical islanding options with three islands comprising 5, 12, and 13 buses. For the highest level of severity (100), the model selects the maximum possible number of islands as the best solution. It is interesting to note how the model responds as the upper bound increases for any given level of severity. For example, for $\alpha = 100$, the model chooses 2, 3, 4, 4 islands for respective upper bounds of 2, 3, 4, 5. Between the bounds of 4 and 5, the model solution does not change. Another observation that can be made that for upper bound of 3 and $\alpha = 70$ and 100, the model selects the maximum number of islands in both cases. But, for the higher level of severity (100), it chooses a different configuration of the islands where the maximum island size is reduced (from 13 to 11) while allowing a higher load reduction (41 to 58 MW).

Table II presents further details of the optimal islanding solutions with actual bus numbers for all twenty test scenarios. Results of some of the scenarios (upper bound 4 and severity levels 30, 50, and 100) are depicted in the Figures 1, 2, and 3.

We also applied our islanding model on the Great Britain (GB) transmission network represented by a reduced 29-bus model [18]. The 29-bus network consists of 99 transmission lines comprising both single and double circuit lines and

TABLE I: Optimal islanding and corresponding load reduction for IEEE 30-bus network under increasing extreme event severity

		Extreme event severity parameter α				
		0	30	50	70	100
Upper bound for the no. of islands	2	30 (0)	12,18 (24)	15,15 (37)	15,15 (37)	15,15 (37)
	3	30 (0)	12,18 (24)	5,12,13 (41)	5,12,13 (41)	10,9,11 (58)
	4	30 (0)	12,18 (24)	5,12,13 (41)	5,12,13 (41)	3,9,9,9 (67)
	5	30 (0)	12,18 (24)	5,12,13 (41)	9,9,12 (49)	3,9,9,9 (67)

Note: 12,18 (24) indicates two islands with 12 and 18 buses and a load reduction of 24 MW.

TABLE II: Recommended Islanding of IEEE 30-Bus Network for Various Upper Bound and Severity Combinations

		Extreme event severity parameter α				
		0	30	50	70	100
Upper bound for the no.of islands	2	**I1:**1-30	**I1:**2,5-11,20-22,28 **I2:**1,3,4,12-19,23-27,29,30	**I1:**2,5-11,20-22,27-30 **I2:**1,3,4,12-19,23-26	**I1:**2,5-11,20-22,27-30 **I2:**1,3,4,12-19,23-26	**I1:**2,5-11,20-22,27-30 **I2:**1,3,4,12-19,23-26
	3	**I1:**1-30	**I1:**2,5-11,20-22,28 **I2:**1,3,4,12-19,23-27,29,30	**I1:**25-27,29,30 **I2:**1,3,4,12-19,23,24 **I3:**2,5-11,20-22,28	**I1:**25-27,29,30 **I2:**1,3,4,12-19,23,24 **I3:**2,5-11,20-22,28	**I1:**9-11,17,20-22,24-26 **I2:**1,3,4,12-16,18,19,23 **I3:**2,5-8,27-30
	4	**I1:**1-30	**I1:**2,5-11,20-22,28 **I2:**1,3,4,12-19,23-27,29,30	**I1:**25-27,29,30 **I2:**1,3,4,12-19,23,24 **I3:**2,5-11,20-22,28	**I1:**25-27,29,30 **I2:**1,3,4,12-19,23,24 **I3:**2,5-11,20-22,28	**I1:**12-16,18-20,23 **I2:**1,3,4,6,8,27-30 **I3:**9-11,17,21,22,24-26 **I4:**2,5,7
	5	**I1:**1-30	**I1:**2,5-11,20-22,28 **I2:**1,3,4,12-19,23-27,29,30	**I1:**25-27,29,30 **I2:**1,3,4,12-19,23,24 **I3:**2,5-11,20-22,28	**I1:**1,3,4,12-19,23 **I2:**2,5-8,27-30 **I3:**9-11,20-22,24-26	**I1:**9-11,20-22,24-26 **I2:**1,3,4,6,8,27-30 **I3:**12-19,23 **I4:**2,5,7

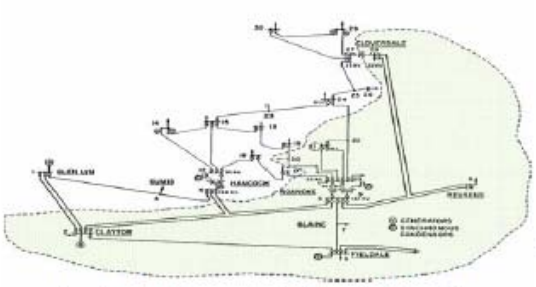

Fig. 1: Islanded scenarios for K = 4 and α = 30

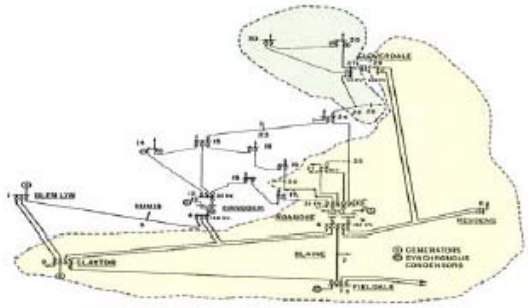

Fig. 2: Islanded scenarios for K = 4 and α = 50

serving a total load of 56 GW. The network has generator(s) in most of its buses and its total generation capacity far exceeds the demand. Consequently, for most of the reasonable islanding options for this network, there are no load reductions. Hence, to adequately test our islanding model, we assigned the generators to a smaller subset of the buses and reduced the total generating capacity to slightly above the demand, as described next. Generators are considered to be at buses 1, 6, 12, 18, and 27 with maximum capacities of 8.6, 13.2, 13.8, 9.3, and 11.5 GW, respectively. The anticipated severity of the extreme event parameter α is assumed to be between 0 and 1000, and the parameter c_{il} of the objective function is considered to be 1. The results are presented in Table III. It may be noted that the performance of the model in 29-bus GB network is similar to that observed for the IEEE 30 bus network. Depending on the severity level, the model often recommends options where the number of islands is lower than a predefined maximum number.

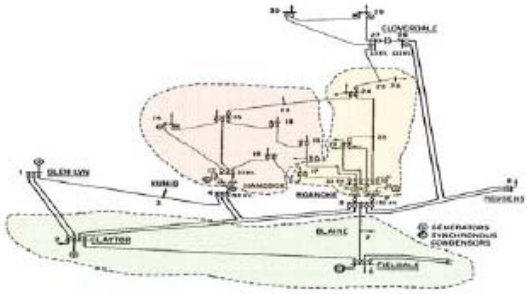

Fig. 3: Islanded scenarios for K = 4 and α = 100

VI. Conclusions

Power grids are becoming more interconnected to cope with growing demand and market restructuring, among others. This is making the grids more vulnerable to cascading failures during extreme events. Therefore, it is essential to develop self healing strategies, like islanding, which has been a topic of study for nearly a decade. Various islanding methods have been presented to the literature. However, most of the existing methods are limited to forming either just two islands or a prespecified number of islands. None, to our knowledge, determine an optimal level of islanding considering the anticipated severity of an extreme event. This paper attempts to fill this gap. Our MIP model considers anticipated severity of the event

TABLE III: Optimal islanding and corresponding load reduction for reduced 29-bus GB transmission network under increasing extreme event severity

		Extreme event severity parameter α				
		0	300	500	700	1000
Upper bound for the no. of islands	2	29 (0)	17,12 (486)	17,12 (486)	13,16 (988)	13,16 (988)
	3	29 (0)	8,12,9 (769)	8,9,12 (769)	9,11,9 (1271)	11,9,9 (1271)
	4	29 (0)	8,12,9 (769)	9,8,12 (769)	5,8,8,8 (1578)	8,5,8,8 (1578)

Note: 9,8,12 (769) indicates three islands with 9, 8, and 12 buses and a load reduction of 769 MW.

related parameter α as an input, which has not been considered earlier. We demonstrate via the IEEE 30-bus network that if a high value of upper bound for the number of islands is chosen, the model determines the appropriate number of islands based on the severity.

While severity related parameter (α) in the model helps to incorporate a measure of cost from the extreme event, we have not presented a method to assess its value. We believe that the two primary cost components of the value of α would be the cost of network recovery and the cost of unplanned load loss. Higher the severity of an event higher will be the value of α. Also, we have made a sweeping assumption that all the generators across the network are coherent, which may not be practical. In that case, additional constraints will have to be added which will likely lead to higher computational complexity. Finally, as in the literature, we have used the DC power flow model that fails to address the reactive power balance. Hence, in practice, we may have to deviate from the optimal islanding solutions provided by our model to ensure voltage stability.

REFERENCES

[1] Kenward, Alyson, and Urooj Raja. "Blackout: Extreme weather, climate change and power outages." Climate Central (2014): 1-23.

[2] National Academies of Sciences, Engineering, and Medicine. Attribution of extreme weather events in the context of climate change. National Academies Press, 2016.

[3] Keogh, Miles, and Christina Cody. "The National Association of Regulatory Utility Commissioners." (2012).

[4] Technology Innovation, "Electric Power System Flexibility: Challenges and Opportunities", EPRI, Palo Alto, CA: Feb 2016, 3002007374, https://www.epri.com/#/pages/product/3002007374/

[12] Trodden, P. A., et al. "MILP islanding of power networks by bus splitting." Power and Energy Society General Meeting, 2012 IEEE. IEEE, 2012.

[5] Technology Innovation, "Electric Power System Connectivity: Challenges and Opportunities", EPRI, Palo Alto, CA: Feb 2016, 3002007375, https://www.epri.com/#/pages/product/3002007375/

[6] Panteli, Mathaios, and Pierluigi Mancarella. "Influence of extreme weather and climate change on the resilience of power systems: Impacts and possible mitigation strategies." Electric Power Systems Research 127 (2015): 259-270.

[7] You, Haibo, Vijay Vittal, and Xiaoming Wang. "Slow coherency-based islanding." IEEE Transactions on Power Systems 19.1 (2004): 483-491.

[8] Yusof, S. B., G. J. Rogers, and R. T. H. Alden. "Slow coherency based network partitioning including load buses." IEEE Transactions on Power Systems 8.3 (1993): 1375-1382.

[9] Xu, Guangyue, and Vijay Vittal. "Slow coherency based cutset determination algorithm for large power systems." IEEE Transactions on Power Systems 25.2 (2010): 877-884.

[10] Sun, Kai, Da-Zhong Zheng, and Qiang Lu. "Splitting strategies for islanding operation of large-scale power systems using OBDD-based methods." IEEE transactions on Power Systems 18.2 (2003): 912-923.

[11] Fan, Neng, et al. "A mixed integer programming approach for optimal power grid intentional islanding." Energy Systems 3.1 (2012): 77-93.

[13] Pahwa, Sakshi, M. Youssef, P. Schumm, C. Scoglio, and N. Schulz. "Optimal intentional islanding to enhance the robustness of power grid networks." Physica A: Statistical Mechanics and its Applications 392, no. 17 (2013): 3741-3754.

[14] Ding, Lei, et al. "Two-step spectral clustering controlled islanding algorithm." IEEE Transactions on Power Systems 28.1 (2013): 75-84.

[15] Liu, Wenxin, et al. "Binary Particle Swarm Optimization Based Defensive Islanding Of Large Scale Power Systems." IJCSA 4.3 (2007): 69-83

[16] Dilkina, Bistra N., and Carla P. Gomes. "Solving Connected Subgraph Problems in Wildlife Conservation." CPAIOR. Vol. 6140. 2010.

[17] Amraee, Turaj, and Hossein Saberi. "Controlled islanding using transmission switching and load shedding for enhancing power grid resilience." International Journal of Electrical Power & Energy Systems 91 (2017): 135-143.

[18] M. Belivanis and K. Bell. Representative GB network model: Notes. Univ. Strathclyde, Glasgow, U.K., 2011.